
THORLABS

Discovery

EDU-MINT2 EDU-MINT2/M Michelson Interferometer Kit

User Guide



Table of Contents
















Chapter 1	Warning Symbol Definitions.....	1
Chapter 2	Safety	2
Chapter 3	Description	3
Chapter 4	Kit Components	4
4.1	<i>Basic Components of the Interferometer</i>	<i>4</i>
4.2	<i>Components to Observe the 2nd Interferometer Output ..</i>	<i>6</i>
4.3	<i>Components for the Refractive Index Measurement.....</i>	<i>6</i>
4.4	<i>Components for Interference with LEDs.....</i>	<i>7</i>
4.5	<i>Components for the Thermal Expansion Setup</i>	<i>8</i>
4.6	<i>Imperial Kit Hardware.....</i>	<i>9</i>
4.7	<i>Metric Kit Hardware</i>	<i>9</i>
Chapter 5	Setup and Adjustment.....	10
5.1	<i>Assembling the Components</i>	<i>10</i>
5.2	<i>Setting Up and Adjusting the Michelson Interferometer</i>	<i>13</i>
Chapter 6	Theoretical Background.....	18
6.1	<i>Interference using the Michelson Interferometer</i>	<i>18</i>
6.2	<i>Determining the Wavelength.....</i>	<i>22</i>
6.3	<i>Coherence.....</i>	<i>23</i>
6.4	<i>Interferometric Determination of the Refractive Index .</i>	<i>27</i>
6.5	<i>Determining a Thermal Expansion Coefficient.....</i>	<i>28</i>
6.6	<i>Using the Interferometer as a Spectrometer</i>	<i>29</i>
Chapter 7	Experiments and Examples	31
7.1	<i>Preliminary Tests</i>	<i>31</i>
7.2	<i>Determining the Laser Wavelength.....</i>	<i>33</i>
7.3	<i>Using the Interferometer as a Spectrometer</i>	<i>34</i>

7.4	<i>Interference with LEDs, Coherence</i>	35
7.5	<i>Refractive Index Determination</i>	38
7.6	<i>Thermal Expansion Coefficient</i>	40
Chapter 8	Experiment Overview	43
Chapter 9	Questions	45
Chapter 10	Ideas for Additional Experiments	46
Chapter 11	Modern Michelson Interferometry – LIGO.....	51
Chapter 12	Troubleshooting	52
Chapter 13	Appendix	54
Chapter 14	Regulatory	56
Chapter 15	Thorlabs Worldwide Contacts.....	57



Chapter 1 Warning Symbol Definitions

Below is a list of warning symbols you may encounter in this manual or on your device.

Symbol	Description
	Direct Current
	Alternating Current
	Both Direct and Alternating Current
	Earth Ground Terminal
	Protective Conductor Terminal
	Frame or Chassis Terminal
	Equipotentiality
	On (Supply)
	Off (Supply)
	In Position of a Bi-Stable Push Control
	Out Position of a Bi-Stable Push Control
	Caution: Risk of Electric Shock
	Caution: Hot Surface
	Caution: Risk of Danger
	Warning: Laser Radiation

Chapter 2 Safety



WARNING



The laser module is a class 2 laser, which does not require any protective eyewear. However, to avoid injury, do not look directly into the laser beam.

LASER RADIATION

DO NOT STARE INTO BEAM
CLASS 2 LASER PRODUCT

Chapter 3 Description

The objective of this experiment package is to become familiar with the interferometer as a highly sensitive measuring instrument. Since the applications in technology and industry are extremely diverse, this package includes various experiments that highlight different aspects of physics.

First a straightforward Michelson interferometer is built. It is distinguished by its ease of adjustment, compared for example to the Mach-Zehnder interferometer. In particular, the influence of the interferometer's arm length on the interference pattern is discussed. This section also demonstrates how an interferometer can serve as a spectrometer.

The topic of coherence takes center stage in the next step. Initially, an interference pattern is generated with a narrow-band red LED. If the interferometer is adjusted precisely enough, one can replace the red LED with a white one which allows white light interference to be observed within the coherence length.

Determining the refractive index of a Plexiglas plate is the object of another experiment. Here, a Plexiglas plate is positioned in an arm of the interferometer and rotated. The rotation increases the optical path of the laser in this arm, so that the interference pattern shows characteristic light-dark transitions (swelling / disappearance of rings). Then the refractive index is determined based on their number, the plate thickness, and the rotation angle.

The final experiment illustrates how even extremely slight expansion can be measured with an interferometer. Here a metal rod to which an interferometer mirror has been attached is heated so that it expands. Expansion in turn results in light-dark transitions. The expansion coefficient can be calculated from the number of light-dark transitions and the temperature of the rod.

This Michelson interferometer setup therefore opens up a wide range of possibilities to become familiar with various fields of application for interferometry. In particular, a broad spectrum of phenomena is discussed ranging from interference, coherence, and refraction to the expansion of solids.

Chapter 4 Kit Components

In cases where the metric and imperial kits contain parts with different item numbers, metric part numbers and measurements are indicated by parentheses unless otherwise noted.

4.1 Basic Components of the Interferometer



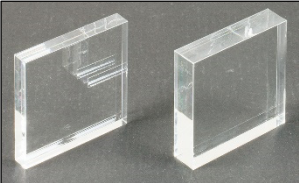
 <p>1 x B1218FX (B3045AX) Steel Breadboard, 12" x 18" (30 cm x 45 cm)</p>	 <p>1 x RDF1 Rubber Dampening Feet, Set of 4</p>	 <p>1 x CPS532-C2 Collimated Laser Diode Module, 532 nm, Class II, Round Beam</p>
 <p>1 x LDS5(-EC) 5 VDC Regulated Power Supply, 2.5 mm Phono Plug, 120 VAC (230 VAC)</p>	 <p>1 x AD11NT Ø1" Unthreaded Adapter for Ø11 mm Components</p>	 <p>2 x KM100 Ø1" Mirror Mount</p>
 <p>2 x PF10-03-P01 Ø1" Protected Silver Mirror</p>	 <p>1 x SM1ZP(M) Z-Axis Translation Mount</p>	 <p>1 x BA2S5(M) Spacer, 2" x 3" (50 mm x 75 mm), 0.250" (6.25 mm) Thick</p>

 <p>2 x BA2(/M) Base, 2" x 3" x 3/8" (50 mm x 75 mm x 10 mm)</p>	 <p>1 x EDU-VS1(/M) Plastic Viewing Screen</p>	 <p>1 x LMR1(/M) Ø1" Lens Mount</p>
 <p>1 x LB1471 N-BK7 Bi-Convex Lens, Ø1", f = 50.0 mm, Uncoated</p>	 <p>1 x CCM1-BS013(/M) Non-Polarizing Beamsplitter Cube, 400 - 700 nm</p>	 <p>4 x UPH1.5 (UPH30/M) 1.5" (30 mm) Long Universal Post Holder</p>
 <p>4 x TR1.5 (2 x TR30/M + 2 x TR40/M) Ø1/2" (Ø12.7 mm) Post, 1.5" (2 x 30 mm, 2 x 40 mm)</p>		

4.2 Components to Observe the 2nd Interferometer Output

 <p>1 x EBS1 Ø1" Economy Beamsplitter</p>	 <p>1 x LMR1(M) Ø1" Lens Mount</p>	 <p>1 x TR1.5 (TR40/M) Ø1/2" (Ø12.7 mm) Post, 1.5" (40 mm) Long</p>
---	--	---

4.3 Components for the Refractive Index Measurement

 <p>1 x PR01(M) High-Precision Rotation Mount</p>	 <p>1 x FP01 General Purpose Plate Holder</p>	 <p>Plexiglas® Plates 8 mm and 12 mm Thick</p>
---	---	---


4.4 Components for Interference with LEDs

 <p>2 x LED631E 635 nm LED, 4 mW, 20° Half Viewing Angle, 10 nm FWHM</p>	 <p>1 x LEDW7E White Light LED, 15 mW, 7.5° Half Viewing Angle, Pack of 5</p>	 <p>2 x LEDMT1F USB-Powered LED Mount, 62 Ω Resistor, USB to Micro-B USB Cable Included</p>
 <p>1 x UPH1.5 (UPH40/M) 1.5" (40 mm) Long Universal Post Holder</p>	 <p>2 x TR1.5 (TR40/M) Ø1/2" (Ø12.7) mm Post, 1.5" (40 mm) Long</p>	 <p>1 x DS5 5 VDC USB Power Supply</p>
 <p>1 x USB-C-72 72" USB 2.0 Type-A Extension Cable</p>	 <p>2 x SMR05(/M) SM05 Lens Mount without Retaining Lip for Ø1/2" Optics</p>	 <p>2 x SM05L03 SM05 Lens Tube, 0.30" Thread Depth, Retaining Ring included</p>
 <p>1 x Ruler, 12" (30 cm)</p>		


4.5 Components for the Thermal Expansion Setup

 <p>1 x MH25 Mirror Holder for Ø1", 2.5 to 6.1 mm Thick Optics</p>	 <p>1 x ME1-G01 Ø1" Aluminum Mirror</p>	 <p>1 x Aluminum Post Ø12.7 mm, 90 mm Long, Tap Accepts MH25</p>
 <p>1 x RA90(M) Right-Angle Post Clamp, Fixed 90° Adapter</p>	 <p>1 x TR2 (TR50/M) Ø1/2" (Ø12.7 mm) Post, 2" (50 mm) Long</p>	 <p>1 x PH1.5 (PH40/M) 1.5" (40 mm) Long Post Holder</p>
 <p>1 x BA1S(M) Base, 1" x 2.3" x 3/8" (25 mm x 58 mm x 10 mm)</p>	 <p>1 x Digital Thermometer</p>	 <p>1 x Sensor</p>
 <p>1 x Flexible Polyimide Foil Heater with 10 kΩ Thermistor and Added Banana Plugs</p>	 <p>1 x Electrical Tape, 10 m Long</p>	

4.6 Imperial Kit Hardware

Type	Quantity	Type	Quantity
1/4"-20 x 1/4" Cap Screw	2	6-32 x 1/4" Cap Screw	1
1/4"-20 x 3/8" Cap Screw	1	8-32 x 3/8" Cap Screw	1
1/4"-20 x 1/2" Cap Screw	4	8-32 x 5/8" Cap Screw	3
1/4"-20 x 5/8" Cap Screw	9	1/4" Washer	15
1/4"-20 x 3/4" Cap Screw	4	1/4" Counterbore Adapter for #8 Screws	4
1 x 5/64" Hex Key, 1 x 7/64" Hex Key, 1 x 1/16" Hex Key, 1 x 9/64" Hex Key		 1 x BD-3/16L Balldriver for 1/4"-20 Cap Screws	

4.7 Metric Kit Hardware

Type	Quantity	Type	Quantity
M6 x 8 mm Cap Screw	2	M4 x 6 mm Cap Screw	1
M6 x 10 mm Cap Screw	1	M4 x 10 mm Cap Screw	1
M6 x 12 mm Cap Screw	4	M4 x 16 mm Cap Screw	3
M6 x 16 mm Cap Screw	9	M6 Washer	15
M6 x 20 mm Cap Screw	4	M6 Counterbore Adapter for M4 Screws	4
1 x 1.5 mm Hex Key, 1 x 2 mm Hex Key, 1 x 3 mm Hex Key		 1 x BD-5ML Balldriver for M6 Cap Screws	

Chapter 5 Setup and Adjustment

This chapter discusses how to assemble the various components and explains how to set up and adjust the interferometer.

5.1 Assembling the Components

First screw the four rubber feet to the four holes in the bottom of the breadboard using the 1/4"-20 x 1/2" (M6 x 12 mm) screws. Now assemble the various parts of the setup:

Screen



Components:
EDU-VS1(/M) Screen
BA2(/M) Base

Lens



Components:
LB1471 Lens
LMR1(/M) Lens Mount
TR1.5 (TR40/M) Post
UPH1.5 (UPH30/M)
 Universal Post Holder

Mirror



Components:
PF10-03-P01 Mirror
KM100 Mirror Mount
TR1.5 (TR30/M) Post
UPH1.5 (UPH30/M)
 Universal Post Holder

Screen Assembly: First, screw the screen onto the BA2(/M) base using a counterbore adapter and the 8-32 x 3/8" (M4 x 10 mm) cap screw.

Lens and Mirror Assembly: Screw the 1.5" (40 mm) long post into the lens holder and place it in the universal post holder. To insert the lens, first remove the retaining ring, then insert the lens and screw the retaining ring back into place. The mirror is installed in the KM100 mirror holder in a similar fashion. To mount the holder on the post, proceed as shown in the photos that follow.



The mirror is locked in place using the nylon-tipped setscrew. Now you need to assemble the laser, beamsplitter and movable mirror as additional components of the setup.

Laser

Beamsplitter

Movable Mirror



Components:
CPS532-C2 Laser
KM100 Mount
AD11NT Adapter
TR1.5 (TR30/M) Post
UPH1.5 (UPH30/M)
 Universal Post Holder

Components:
CCM1-BS013(/M)
 Beamsplitter Cube
TR1.5 (TR40/M) Post
UPH1.5 (UPH30/M)
 Universal Post Holder

Components:
PF10-03-P01 Mirror
SM1ZP(/M) Stage
BA2(/M) Base
BA2S5(/M) Spacer

Laser: Screw the KM100 mount onto the post as shown above. Then place the laser in the adapter and lock it using the two screws. Finally, insert the adapter into the KM100 and lock it using the nylon-tipped setscrew. Connect the laser to the LDS5(-EC) power supply and check the bottom of the LDS5(-EC) to make sure the correct voltage is used.

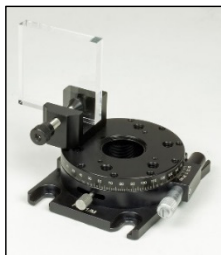
Beamsplitter: The beamsplitter cube is screwed onto the 1.5" (40 mm) long post. For the imperial kit, use the thread adapter provided with the cube.

Movable Mirror: To mount the SM1ZP(/M) stage, put it on the BA2S5(/M) spacer and the BA2(/M) base (at the bottom). Secure the stage by using three counterbore adapters and three 8-32 x 5/8" (M4 x 16 mm) cap screws. Secure the mirror in the stage by removing one retaining ring, placing the mirror in the mount, and screwing the retaining ring back in its place.

The elements installed so far are the basic components of the interferometer. The next set of components will be used with the interferometer in the various experiments explained in this manual.

Ø1" Beamsplitter: To assemble the second beamsplitter, remove the retaining ring from the LMR1(/M) mount, place the beamsplitter in the mount and attach the retaining ring. Wear gloves while touching the beamsplitter. Screw the beamsplitter mount onto a TR1.5 (TR40/M) post.

Rotation Platform



Components:
PR01(/M) Rotation Stage
FP01 Universal Filter Mount
 Plexiglas Plate

LED Mount



Components:
 LED
LEDMT1F LED Mount
SM05L03 Lens Tube
SMR05(/M) Lens Mount
TR1.5 (TR40/M) Post
UPH1.5 (UPH40/M)
 Universal Post Holder
DS5 Power Supply
USB-C-72 USB Extension
 Cable

Thermal Expansion

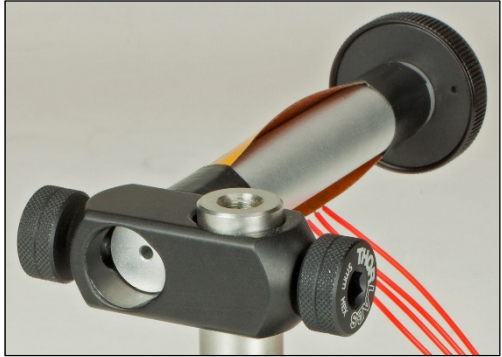


Components:
ME1-G01 Mirror
MH25 Mirror Holder
 Aluminum Rod
 Foil Heater + Tape
RA90(/M) 90° Adapter
TR2 (TR50/M) Post
PH1.5 (PH40/M) Post Holder
BA1S(/M) Base

Rotation Platform: First, attach the universal filter mount to the outer part of the stage using a 6-32 x 1/4" (M4 x 6 mm) cap screw. Next, insert the thin Plexiglas plate. **Make sure to remove the protective films from both sides of both Plexiglas plates.**

LED Mount: For the component with the LED, screw the SMR05 Lens Mount to the post with its 8-32 (M4) set screw and place it in the post holder. The contacting leads of the LED have to be cut to the correct length to make it compatible to the USB-Powered LED holder. Use pincers or scissors to cut the longer lead to 6 mm and the shorter lead to 5 mm. When connecting the LED to the LEDMT1F mount, plug the longer lead into the socket marked with a plus sign and the shorter lead into the socket marked with a minus sign. The length and polarity of the contacts is also marked on the side of the LEDMT1F mount. Apply only light force and make sure to use the correct polarity when inserting the LED! Connect a red LED631E to one LEDMT1F and a white LEDW7E to the other one. We recommend marking the LED holders to facilitate identification of the LED color later on. Screw the LEDMT1F into the SMR05 lens mount from one side. Then screw the

SM05L03 lens tube in from the other side. The addition of the lens tube helps to block light emitted by the LED at large angles from reaching the screen. To operate the LED, connect the LEDMT1F to the DS5 power supply via the USB to micro-B USB cable and use the USB extension cable if needed. To switch between the LED colors, take the post with the LEDMT1F out of the post holder and insert the post with the second LEDMT1F component.



Thermal Expansion: Finally, assemble the setup for the thermal expansion experiment. Screw the BA1S(/M) base onto the post holder with a 1/4"-20 x 3/8" (M6 x 10 mm) cap screw. Place the 2" (50 mm) post into the post holder facing upside down. Attach the 90° adapter and place the aluminum rod in it. **Orient the rod so that the end with the unthreaded hole is in the 90° adapter; the threaded hole needs to point away from the adapter. The end face of the aluminum post should be aligned right below the screw of the RA90(/M), as shown in the photo above.** Remove the protective film from the foil heater and carefully affix it to the rod using the provided tape. Finally, place the mirror into the mirror holder and screw it onto the aluminum rod.

5.2 Setting Up and Adjusting the Michelson Interferometer

In the Michelson interferometer, a laser beam is split by a 50:50 beamsplitter; the split beams are then reflected back by mirrors and recombined at the beamsplitter. A screen at the output of the interferometer shows an interference pattern. A lens is used to diverge the beam in order to obtain an interference pattern consisting of light and dark rings (constructive or destructive interference, respectively). To set up the interferometer, follow these steps:

1. First, position the translatable mirror assembly at the edge of the breadboard using four 1/4"-20 x 3/4" (M6 x 20 mm) cap screws.
2. Position the laser assembly on the opposing side of the breadboard. Now tip and tilt the laser so that the reflected beam falls back into the laser aperture. You may need to move the laser in order to hit the center of the mirror. After that, secure the base to the breadboard with a 1/4"-20 x 5/8" (M6 x 16 mm) cap screw.



WARNING



The laser module is a class 2 laser, which does not require any protective eyewear. However, to avoid injury, do not look directly into the laser beam.

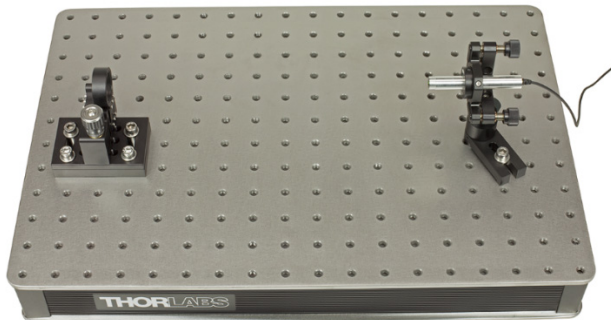


Figure 1 Placing the Laser and the First Mirror

3. Install the beamsplitter and the screen. Ensure that the beam is split at a 90° angle. This can be achieved by observing the secondary reflections on the screen. When they coincide with the primary reflection, the beamsplitter is at a 90° angle.

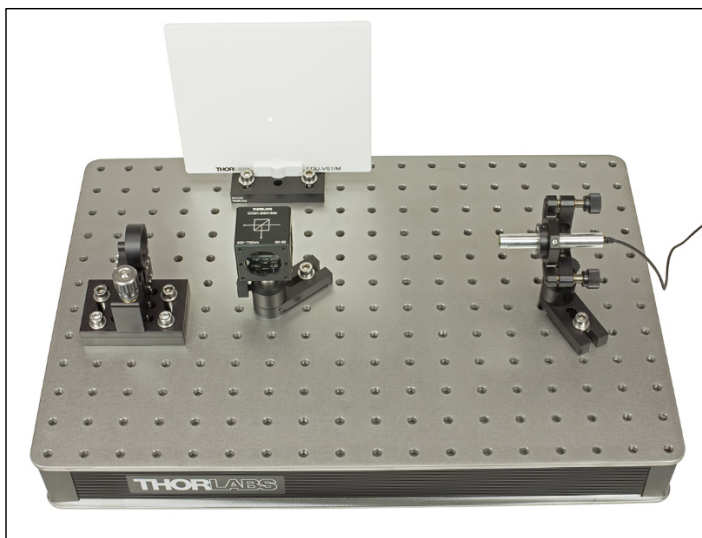


Figure 2 Placing the Beamsplitter

It is possible that a slight deviation occurs in the vertical direction (as shown in Figure 3). This does not affect the measurements in the experiments. The deviation means that there is a slight tilt among the laser, beam splitter and translation stage. To get rid of it, either the translation stage or the beam splitter would have to be mounted kinematically which in turn would compromise the stability.



Figure 3 Laser spots with misaligned (left) and aligned (right) beamsplitter.

4. Next, install the second mirror. One should ensure that the distance between the beamsplitter and the mirrors is about the same along both interferometer arms.

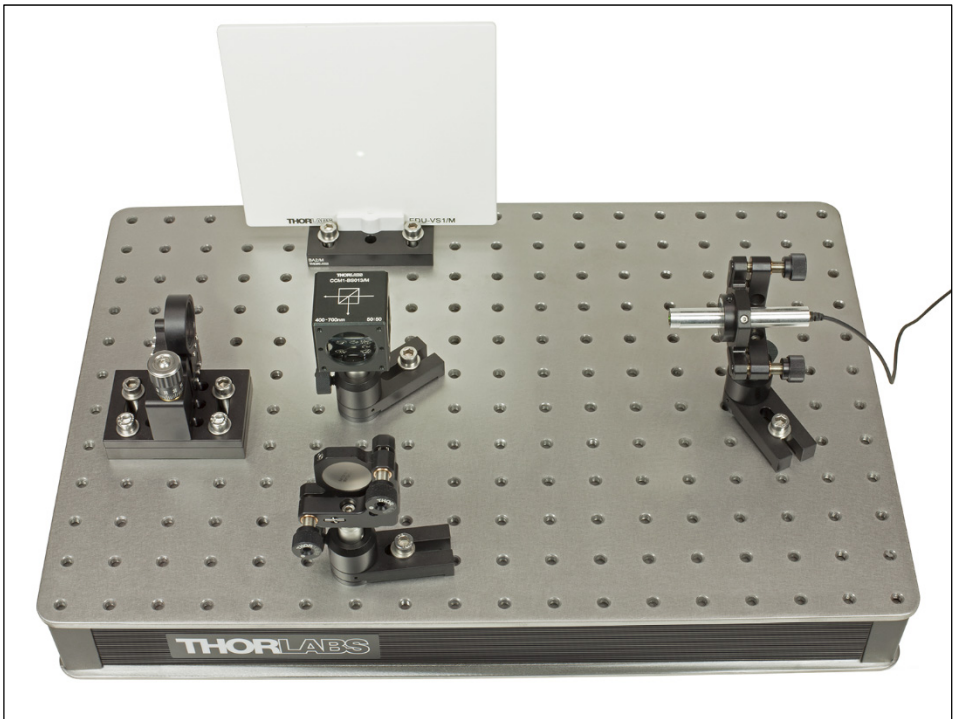


Figure 4 Placement of the Second Mirror

5. You should now see the two partial beams as bright spots on the screen. Tip and tilt the second mirror until they overlap.
6. Finally, place the lens between the laser and the beamsplitter. You may already see interference rings. If not, turn the screws on the adjustment mirror and try to create interference. It may help to move the screen away from the breadboard.

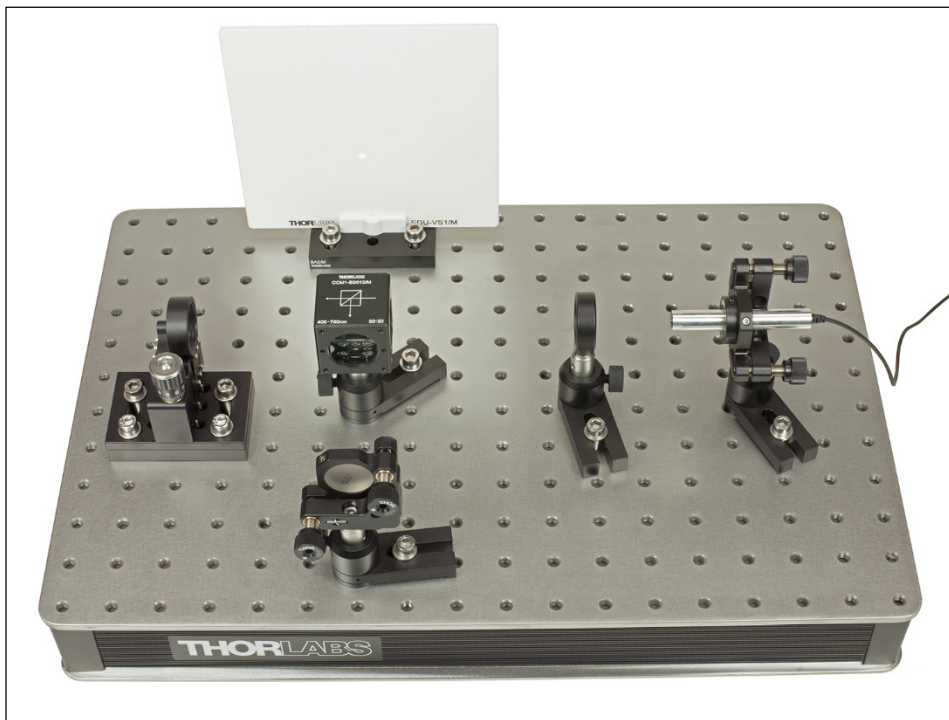


Figure 5 Placement of the Lens to Observe Concentric Circles

7. Placing the lens behind the beamsplitter and moving the screen away from the breadboard (as shown in Figure 6) results in a pattern of stripes instead of rings (as shown in Figure 7). Whether you choose to count rings or stripes is a matter of personal preference.



Figure 6 Alternative Placement of the Lens to Observe Lines

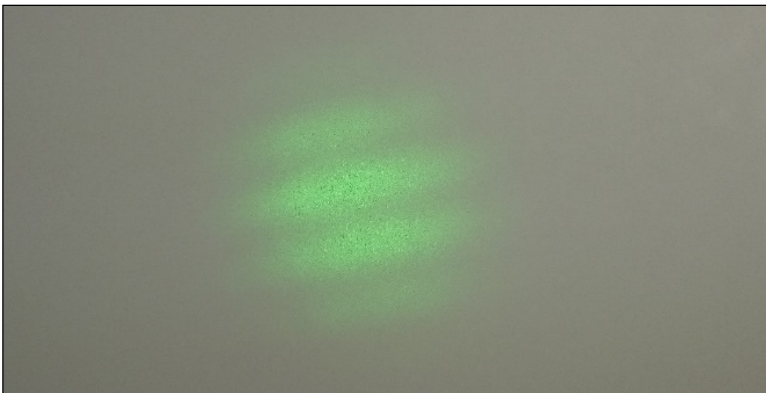


Figure 7 Interference Pattern Produced by the Lens Position Shown in Figure 6

Chapter 6 Theoretical Background

This chapter discusses the essential theoretical foundations that apply to the experiments which follow. The chapter begins with a brief discussion of interference in general and an explanation of the form of the interference pattern. Coherence is discussed next since one experiment involves interference with LEDs. This chapter also explains the theoretical basis for an experiment described later in the manual where the refractive index of a Plexiglas plate is determined. Thermal expansion and the thermal expansion coefficient are addressed at the chapter's conclusion.

6.1 Interference using the Michelson Interferometer

Before building the interferometer, we are first going to examine the underlying theory¹. Initially we represent the situation schematically in Figure 8.

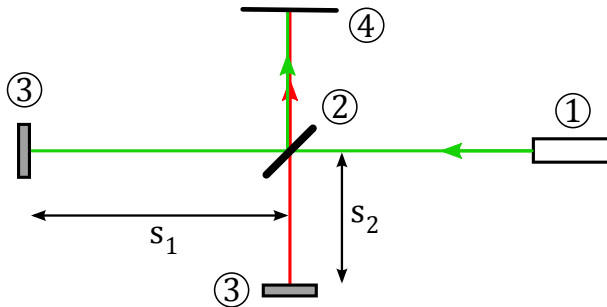


Figure 8 Sketch of a Michelson interferometer. The laser (1) is aimed at the beamsplitter (2) which divides the beam into two partial beams. These are reflected by the respective mirrors (3). An interference pattern can be observed on the screen (4).

The laser is divided by the beamsplitter, and the partial beams reflected by the mirrors overlap again at the beamsplitter. Naturally half the light travels back in the direction of the laser here. We can mathematically describe how the light intensity on the screen depends on the path length difference Δs between the two paths s_1 and s_2 . Limiting ourselves to examining an incident plane wave along the optical axis:

$$E_i = E_0 \cos(\omega t - kx) \tag{1}$$

Here ω is the angular frequency, t the time, k the wave number (i.e., $2\pi/\lambda$), and x the local variable. In the following example, we represent the transmission capacity of the beamsplitter with T and the reflection capacity with R . Now let us examine the amplitude of the partial wave of one interferometer arm at the location of the screen:

$$|E_1| = \sqrt{R \cdot T} \cdot E_0 \cdot \cos(\omega t + \varphi_1) \tag{2}$$

¹ Illustrations on this topic are found in numerous physics textbooks. In the following, we are guided by *Demtröder: Experimentalphysik 2*, 5th edition (2008).

Here φ_1 is the phase, the value of which is established by the actual optical path. The factor $\sqrt{R \cdot T}$ is therefore explained because the beam in path 1 is first transmitted and then reflected. The description of the beam in path 2 is similar, but the beam is first reflected and then transmitted. This results in the same factor and the amplitude of the partial wave of the second interferometer arm is given on the screen by²

$$|\mathbf{E}_2| = \sqrt{R \cdot T} \cdot E_0 \cdot \cos(\omega t + \varphi_2) \quad (3)$$

where φ_2 is the corresponding phase for the second path. The intensity on the screen is then determined by

$$I = c \varepsilon_0 |\mathbf{E}_1 + \mathbf{E}_2|^2 = c \varepsilon_0 R T E_0^2 [\cos(\omega t + \varphi_1) + \cos(\omega t + \varphi_2)]^2. \quad (4)$$

Naturally we only perceive the temporal averaging of the light field oscillation on the screen, so that only the averaging

$$\frac{1}{2\pi} \int_0^{2\pi} [\cos(\omega t + \varphi_1) + \cos(\omega t + \varphi_2)]^2 d(\omega t) = 1 + \cos(\varphi_1 - \varphi_2) \quad (5)$$

is incorporated in the observed intensity. Furthermore, we are going to assume that both the transmission and the reflection capability have the value of 0.5, which is a good approximation for the beamsplitter being used. As the average intensity, we therefore find \bar{I}

$$\bar{I} = \frac{1}{4} c \varepsilon_0 E_0^2 (1 + \cos \Delta\varphi), \quad (6)$$

where the phase difference of the two partial waves translates directly into the path length difference Δs between them:

$$\Delta\varphi = \frac{2\pi}{\lambda} \Delta s \quad (7)$$

Therefore the intensity dependence on the path length difference between the two interferometer arms is described by a cosine function; see Figure 9.

A fundamental question arises though: when the intensity at the screen drops to zero, where does the light and the energy go? This simple question often tricks students. To answer this it's important to recall that there are two outputs of the interferometer: in the direction of screen and in the direction of the laser! So when the intensity at the screen drops to zero, there's constructive interference in the other output path. This means that all energy is propagating in the direction of the laser.

² Here an interesting aside is that the factor $\sqrt{R \cdot T}$ does not apply to the radiation falling back into the laser. The factors of the partial paths are given by $\sqrt{T \cdot T}$ and $\sqrt{R \cdot R}$ in this case.

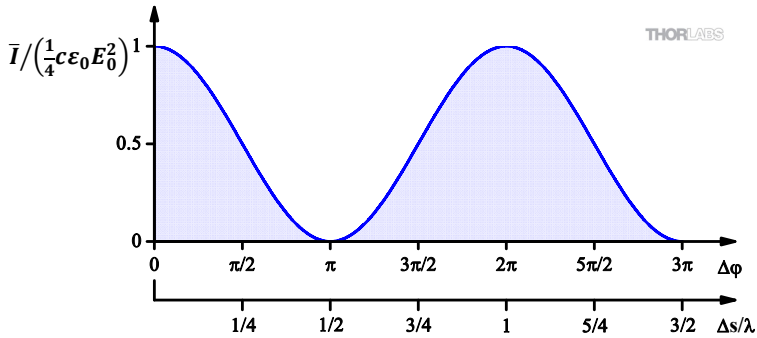


Figure 9 Normalized intensity distribution on the screen depending on the path length difference.

To understand this, one has to look at the phase shifts on a beamsplitter. The cube beamsplitter is composed of two prisms cemented together with a beamsplitter coating applied to the hypotenuse of one of the prisms, as shown in the sketch to the right. When the light travels through the glass and is reflected by the beamsplitter coating, no phase shift occurs. When the light comes from the other direction (with a plate beamsplitter that would correspond to the “air → coating” interface) the phase shift is π (or 180°). Figure 10 shows that the phase shifts between the two interferometer arms differs for each output. Regardless of the mirror position, the two outputs always differ by π which results in complementary patterns.

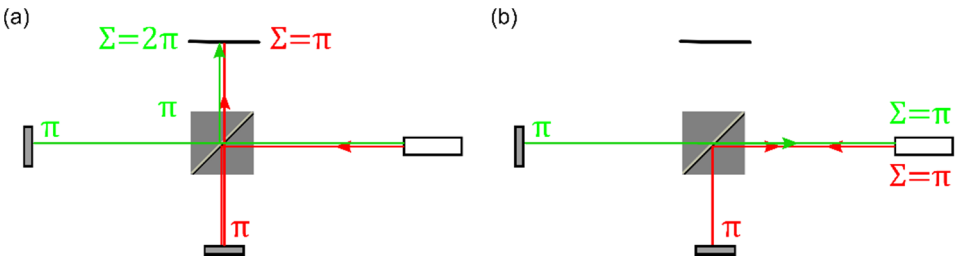
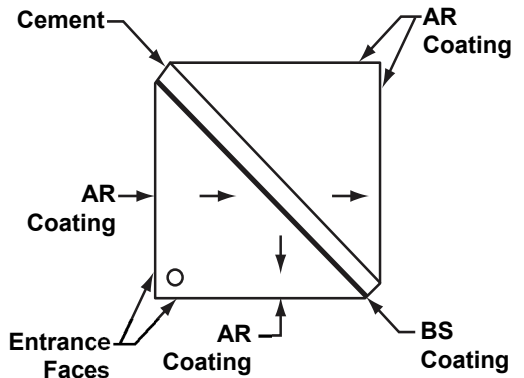


Figure 10 Phase shifts at the beamsplitter coating. Along each optical path, the total phase shift, Σ , is calculated. The two output ports of the interferometer show a relative phase shift that differs by π . This means that the interference patterns are complementary.

Size and Shape of the Pattern

We have now clarified what the interference pattern of a plane wave and/or at the central point looks like. Naturally the real interference pattern appears different than that of a plane wave, since the laser diverges on its way to the screen. This results in a characteristic ring pattern with a size that largely depends on the path length difference Δs . The following brief explanation examines why this is the case and why a ring-shaped pattern forms at all.

When both interferometer arms are not of equal length (which is always the case since it's practically impossible to adjust the interferometer with nanometer precision), then there exist two (virtual) light sources as seen by the screen which correspond to the different light paths through the interferometer. If the path is stretched out in one dimension, one source is behind the other due to the different lengths of the interferometer arms.

As with all interference patterns (such as for the double slit), one can now determine the difference in path length between the path from light source A to point X and the path from light source B to point X (as shown in Figure 11) which then translates to constructive or destructive interference (see Figure 9).

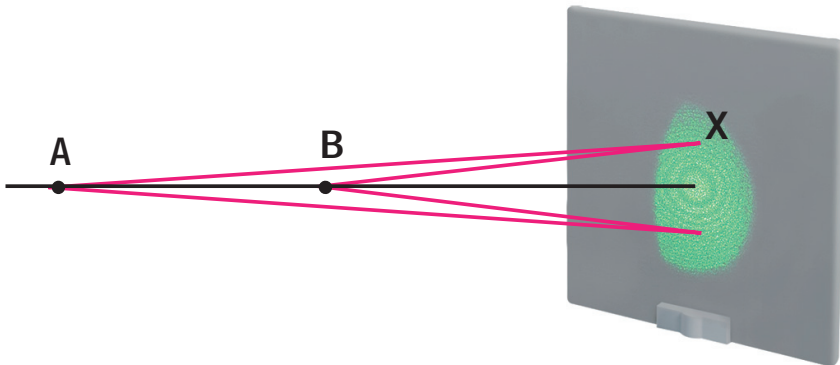


Figure 11 Explanation of a Circular Interference Pattern

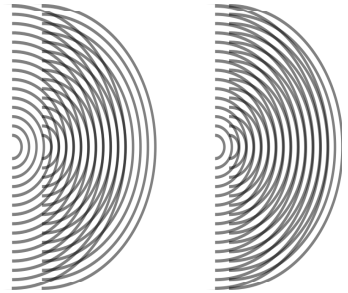
If the arms of the interferometer have very different lengths, the two virtual light sources are far apart. In this case, a small position change on the screen corresponds to a large change in the path length difference, which again translates into a smaller spacing between the fringes. This explains why the interference pattern gets smaller when the interferometer arms have very different lengths.

This line of argument is the same for all points on the screen. Since the lens diverges the beam symmetrically around the optical axis, the interference pattern needs to be symmetric, i.e., concentric, as well.

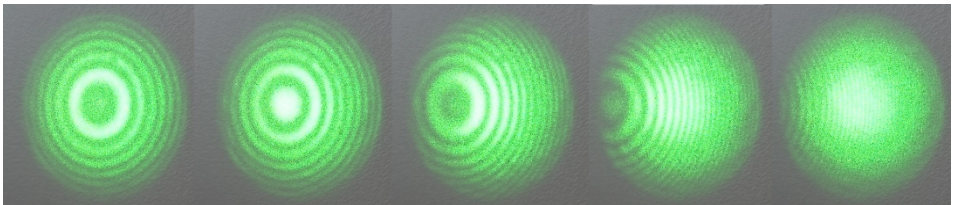
When the two interferometer arms are nearly identical in length, the interference pattern will show very large rings (with the inverse argument from before). This can be used to

adjust the interferometer. In order to find a configuration with nearly identical arm lengths, the central maximum needs to be as large as possible.

A nice way to visualize the ring pattern is to overlap two wavefronts. In practice, we do not have a plane wave but (due to the laser's divergence) a spherical wave. Since the beam is split in two, we have two spherical waves from two virtual sources overlapping. The result is shown in the left sketch. When the centers of the spherical waves move closer together (i.e., the interferometer arms have nearly equal length, right sketch), then the central fringe becomes larger.



When the one of the interferometer's mirrors is tilted, the wavefront from this mirror changes and, thus, alters the interference pattern. The series of photos below shows the pattern when the mirror is rotated with respect to the post axis. On first sight, it looks like the pattern is "moved" to the left. However, this is not quite true, observe the central fringe in the first and second image (dark and bright). So while tilting the mirror, the central fringe changes from bright to dark and bright again several times. Whether a clockwise rotation of the mirror results in a movement of the pattern to the left or to the right depends on which arm of the interferometer is longer.



6.2 Determining the Wavelength

Equation (6) and Figure 9 offer an elegant way to carry out a wavelength measurement. This is most easily realized when the light source emits only one wavelength, such as with a laser. If only one of the mirrors is shifted, the path length difference between the interferometer arms changes and light-dark-light transitions occur in the center, as summarized by the intensity plot in Figure 9.

One therefore shifts the mirror by a defined path Δx and counts the number N of the maximums (or minimums). According to Figure 9, a light-dark-light transition corresponds to a path length difference of λ . However, the light passes along the adjustment path of the mirror twice (on the way there and back), so that the following applies:

$$N \cdot \lambda = 2 \cdot \Delta x \quad \Rightarrow \quad \lambda = \frac{2 \Delta x}{N} \tag{8}$$

6.3 Coherence

The topic of coherence is highly complex. Terms such as the contrast of an interference pattern, correlation functions and the Wiener-Chintschin theorem are essential for a deeper understanding. Therefore only a brief abstract can be provided here, limited to the descriptive values of coherence time and coherence length³.

Coherence in the largest sense describes the capacity of light to create interference. The maximum time span Δt_c , during which the phase differences of random partial waves at a point change by less than 2π , is called the coherence time. If the change falls below 2π , one says that the partial waves are temporally coherent.

What this means is best described with Figure 12.

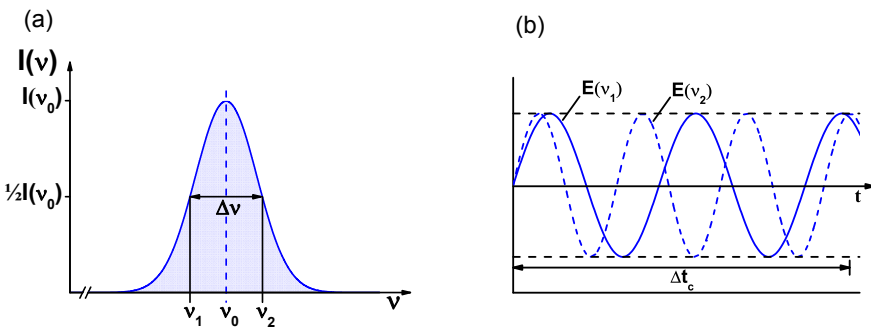


Figure 12 (a) Pulse with spectral width $\Delta\nu$ (FWHM) and (b) the partial waves with frequencies ν_1 and ν_2 after the coherence time Δt_c have a phase offset of 2π .

We imagine a light source with a spectrum as shown in Figure 12(a); its spectral width is denoted by $\Delta\nu$. The source therefore emits light that we can view as the overlapping of various partial waves with frequencies in the interval $[\nu_1 = \nu_0 - 0.5\Delta\nu, \nu_2 = \nu_0 + 0.5\Delta\nu]$. If their phase difference at time $t = 0$ is zero, the maximum phase offset of two partial waves is given by:

$$\Delta\varphi(t) = 2\pi \cdot (\nu_2 - \nu_1) \cdot t \tag{9}$$

If the time span has increased to $1/\Delta\nu$, the phase offset is 2π . This results in the coherence time as:

$$\Delta t_c = \frac{1}{\Delta\nu} \tag{10}$$

The phase offset of the two partial waves with the frequencies ν_1 and ν_2 is shown in Figure 12(b). After the coherence time Δt_c , the offset has increased to 2π . For all other frequency components in the interval $[\nu_1, \nu_2]$, the phase difference is then smaller.

³ Once again we are following *Demtröder: Experimentalphysik 2*, 5th edition (2008).

Linked to the coherence time, the coherence length is ΔL_c . This is the path the light can travel within the coherence time, that is:

$$\Delta L_c = c \cdot \Delta t_c \tag{11}$$

Here the propagation in air was assumed with the refractive index 1. While coherence is a complex topic, the coherence length in case of an interferometer is more straightforward – it corresponds to the path length difference by which the interferometer arms can differ in order to observe interference.

For the practical calculation of the coherence time and/or length, the following approximation is helpful (denotation of the wavelengths similar to Figure 12(a)):

$$\Delta v = \frac{c}{\lambda_1} - \frac{c}{\lambda_2} = \frac{c(\lambda_2 - \lambda_1)}{\lambda_1 \lambda_2} = \frac{c \Delta \lambda}{\lambda_1 \lambda_2} \cong \frac{c \Delta \lambda}{\lambda_0^2} \tag{12}$$

It allows the coherence length of a given spectrum to be estimated approximately by:

$$\Delta L_c \cong \frac{\lambda_0^2}{\Delta \lambda} \tag{13}$$

For a quantitative evaluation of the coherence, one would have to measure the contrast function of the interference pattern⁴. In this experiment package, the coherence length is estimated by shifting one of the mirrors in the interferometer and observing the disappearance of the interference pattern (or the pronounced decrease in contrast).

Selecting the Beamsplitter

When constructing an interferometer, one can in principle choose different types of beamsplitters. The most common types are the plate beamsplitter and beamsplitter cube.

Plate beamsplitters typically consist of a reflective layer applied to a glass substrate, while beamsplitter cubes consist of two prisms cemented together with a layer of beamsplitter coating applied to the hypotenuse of one of the prisms.



Figure 13 Plate and Cube Beamsplitters

For a normal interferometer operated with a laser, it often does not matter which version is chosen. The prices of beamsplitter cubes exceed those of plate beamsplitters and they also differ in their transmission factors. But when one examines white light interference, a problem arises: with a plate beamsplitter, the light traveling through one arm of the interferometer passes through the glass substrate fewer times than the light traveling through the other arm. A method for compensating for this difference is illustrated in Figure 14.

⁴ Note that there are different definitions of coherence. Depending on the definition, the contrast function has to drop to a different value (e.g., $1/e$).

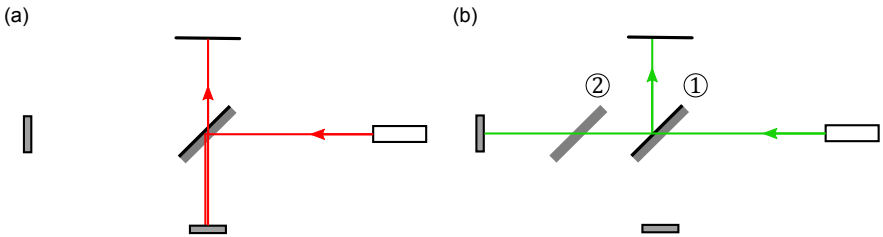


Figure 14 Interferometer with (a) plate beamsplitter and (b) compensator plate (refraction on the surface was disregarded in this sketch)

First let us examine Figure 14(a). Here the laser is reflected off of the beamsplitter when it is inside of the glass substrate, then reflected by the mirror, and finally transmitted through the beamsplitter, therefore propagating through the glass substrate thrice on its way to the screen. In Figure 14(b) it turns out that, without the compensation plate (2), the beam only passes through the glass once since it is reflected on the outside of the beamsplitter on the way back from the mirror to the screen.

This means there is an optical path length difference without the plate (2). If this path length difference is now greater than the coherence length of the light being used, one cannot observe any interference. However, one can counteract this effect with the compensator plate (2) – it consists of the same material as the beamsplitter, only the metal layer is missing. If one now counts how often the partial beams pass through the glass, one notes that both paths pass through the glass substrate the same number of times (thrice).

For a beamsplitter cube, the beam in *each* arm travels through the cube twice. Therefore, no compensator plate is needed, see Figure 15.

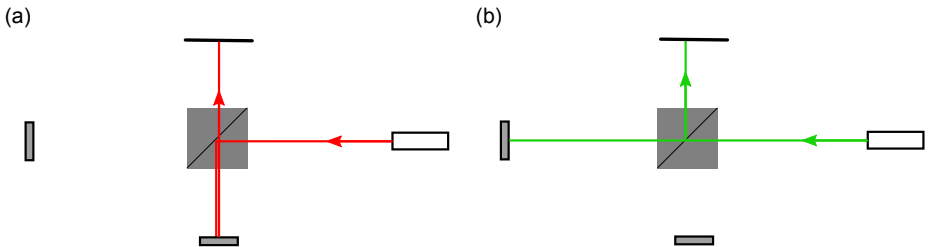


Figure 15 The beam travels through the whole beamsplitter twice for each arm of the interferometer. Thus, no compensation plate is needed with a cube beamsplitter.

Furthermore, one might think that the compensator plate is not needed at all if one shifts one mirror by the correct distance – however this is not the case, since every wavelength “sees” a different optical path due to the dispersion of the glass. This means that shifting the mirror could only compensate for a single wavelength.

A beamsplitter cube is used in this setup instead of the combination of plate beamsplitter and compensator plate, since there is little price difference between the two versions but adjustment with the cube is significantly simpler and more reliable.

Selecting the Mirrors

The surface flatness of the mirrors used in this kit are specified as better than $\lambda/10$, compared to economy mirrors which have a surface flatness of 5λ . It is not absolutely necessary to use this quality of mirror but it provides some advantages.

The difference between the two types of mirrors can be observed when using the white light LED: the quality of the mirrors allows for the white light interference to be observed over a wider range of relative mirror positions. The interference pattern also shows fewer distortions.

White Light Interference Pattern

At first glance, one might expect that the interference pattern comprises concentric circles with the colors of the rainbow. However, this is not the case.

In reality, each point on the screen is illuminated with white light. For most wavelengths, the path difference is neither λ nor $\lambda/2$. However, for a small range of wavelengths the condition for destructive interference is (nearly) met and the intensity on the screen (for these particular wavelengths) is close to zero. Thus, the pattern on the screen is the white light *minus* these few wavelengths. The pattern is, therefore, not colored like a rainbow but made up of subtractive colors.

Also, concentric circles aren't observable. The reason lies in the low coherence length of white light, which requires the difference between the two interferometer arms to be very small. This, in turn, results in a large central maximum (as discussed in Section 6.1: Interference using the Michelson Interferometer). To observe the white light interference pattern, one can adjust the interferometer either (a) so that the central maximum is showing which basically results in a colored maximum or (b) tilt the mirror slightly such that we move away from the central maximum in which case you see colored lines.⁵

⁵ When a gas discharge lamp is used (e.g., a mercury-vapor lamp), the coherence length is a lot higher and the arm difference can be increased. Then, colored, concentric circles can be observed.

6.4 Interferometric Determination of the Refractive Index

Determining the refractive index of a solid (transparent if possible) is one application where a Michelson interferometer can be used as a sensitive measuring instrument. Here the solid is first placed in one arm of the interferometer. Then it is slowly rotated so that the optical path in this interferometer arm changes. This change in the optical path in turn results in a change of the interference pattern. Now the number of light-dark-light transitions, the plate thickness, and the angle of rotation can be used to derive the change in the optical path length, which ultimately allows the refractive index to be determined.

First let us examine the situation when the solid is brought into the light path; see Figure 16(a).

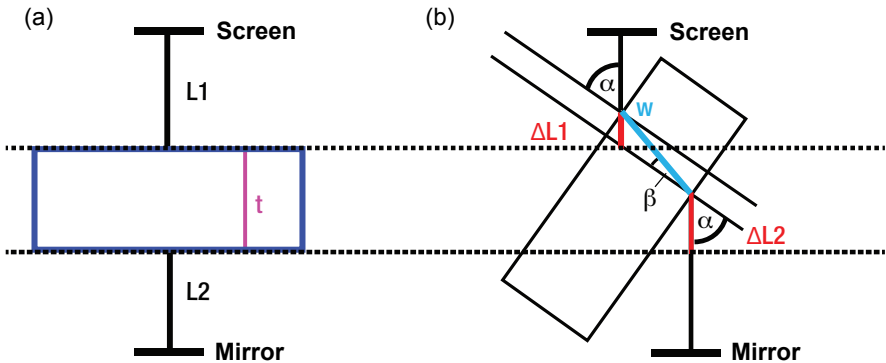


Figure 16 (a) Placing the plate in an interferometer arm (b) Rotation and change in the (optical) path

The length of the physical light path is:

$$\text{Physical path length (not rotated): } L1 + t + L2 \tag{14}$$

On the other hand, the optical path length is given by:

$$\text{Optical path length (not rotated): } L1 + n \cdot t + L2 \tag{15}$$

Here n is the refractive index of the material being examined. The refractive index of the surrounding air is assumed as 1. When the plate is now rotated in the beam, both the physical and the optical paths change; see Figure 16(b). These paths can be described as:

$$\text{Physical path length (rotated): } L1 - \Delta L1 + w + \Delta L2 + L2 \tag{16}$$

$$\text{Optical path length (rotated): } L1 - \Delta L1 + n \cdot w + \Delta L2 + L2 \tag{17}$$

Rotation by the angle α therefore results in the optical path length difference derived from the difference between (17) and (15).

$$\Delta\text{Optical Path} = 2 \cdot (-\Delta L1 + n \cdot w + \Delta L2 - n \cdot t), \quad (18)$$

The factor of 2 appears in the equation because the light passes along the path twice. The path length difference is derived from the light-dark transitions via

$$N \cdot \lambda = \Delta\text{Optical Path} \quad (19)$$

where N denotes the number of transitions.

Now the values $\Delta L1$, $\Delta L2$ and w have to be measured so the refractive index can be determined. This can be studied in detail in Chapter 13; only the resulting equation is given here:

$$n = \frac{\left(\frac{N\lambda}{2t} + \cos \alpha - 1\right)^2 + \sin^2 \alpha}{2\left(-\frac{N\lambda}{2t} - \cos \alpha + 1\right)} \quad (20)$$

6.5 Determining a Thermal Expansion Coefficient

When one increases the temperature of a solid, it will expand in most situations (and depending on the environment). This expansion is described by the thermal expansion coefficient α , which represents the proportionality constant between a relative linear expansion and a corresponding temperature change:

$$\alpha = \frac{1}{L} \frac{dL}{dT} \quad (21)$$

The solution to this equation describes an exponential process, where the length of the solid is given as

$$L = L_0 \cdot \exp(\alpha \cdot \Delta T) \quad (22)$$

Here ΔT is the temperature change of the solid, causing its original length of L_0 to expand to the length L . In first approximation, one can then determine the expansion coefficient with

$$\Delta L \approx \alpha \cdot L_0 \cdot \Delta T \quad (23)$$

where ΔL is the expansion.

This expansion can be examined experimentally by attaching one mirror of the Michelson interferometer to the expanding solid. When the solid expands, the path length difference between the interferometer arms changes, causing the interference pattern to change as well. Then the light-dark-light transitions are measured as with the wave length measurement. When the solid is heated by ΔT and N transitions are measured, the coefficient is derived by

$$\frac{1}{2} N \lambda = \alpha L_0 \Delta T \quad \Rightarrow \quad \alpha = \frac{N \lambda}{2 L_0 \Delta T} \quad (24)$$

where the factor $\frac{1}{2}$ is once again due to the path of the laser to and from the mirror that was shifted.

6.6 Using the Interferometer as a Spectrometer

A very elegant application of an interferometer is to use it as a spectrometer. Assume the light source emits two different wavelengths. Naturally, each wavelength will give rise to its own interference pattern. When these interference patterns overlap well, the contrast of the resulting pattern on the screen is high. This means that the minimum intensity and the maximum intensity of the fringe pattern differ greatly.

However, there exist mirror positions (or path length differences) where the bright fringes of one wavelength overlap with the dark fringes of the other wavelength. This automatically results in a poor contrast. Essentially, the two interference patterns create an effect called beating, meaning that the contrast changes from good to poor and back as a function of the path length difference. The effect can be used to measure the wavelength distance between adjacent spectral lines such as the yellow sodium doublet.

In the following section, we discuss how to determine the wavelength split by observing the contrast as a function of the path difference. We start by recalling Equation (6)

$$\bar{I} \propto \left(1 + \cos\left(\frac{2\pi}{\lambda} \Delta s\right) \right) \quad (25)$$

which states the intensity at the central point of the interference fringes, i.e., on the optical axis. Δs is the path difference between the two interferometer arms (and not the mirror displacement!).

When we have two wavelengths, the total intensity is then given by

$$\bar{I}_{tot} \propto \left(1 + \cos\left(\frac{2\pi}{\lambda_1} \Delta s\right) + 1 + \cos\left(\frac{2\pi}{\lambda_2} \Delta s\right) \right) \quad (26)$$

assuming that the intensities of both spectral components are identical. Equation (26) can be written⁶ as

$$\bar{I}_{tot} \propto \left(2 + 2 \cdot \cos\left(\left(\frac{\pi}{\lambda_1} + \frac{\pi}{\lambda_2}\right) \cdot \Delta s\right) \cdot \cos\left(\left(\frac{\pi}{\lambda_1} - \frac{\pi}{\lambda_2}\right) \cdot \Delta s\right) \right) \quad (27)$$

The interference term vanishes for half-integer multiples of π

$$\left(\frac{\pi}{\lambda_1} - \frac{\pi}{\lambda_2}\right) \cdot \Delta s = (2m + 1) \frac{\pi}{2}, \quad m \in \mathbb{N}_0 \quad (28)$$

⁶ Since $\cos a + \cos b = 2 \cdot \cos(a/2 + b/2) \cdot \cos\left(\frac{a}{2} - \frac{b}{2}\right)$.

which means the contrast becomes zero⁷. Dividing by π and expressing λ_1 and λ_2 as $\lambda_0 \pm \Delta\lambda$ transforms this statement to

$$2 \Delta s = (2m + 1) \frac{\lambda_1 \cdot \lambda_2}{\lambda_2 - \lambda_1} = (2m + 1) \frac{\lambda_0^2 - \Delta\lambda^2}{2 \Delta\lambda} \quad (29)$$

The term $\Delta\lambda^2$ is negligibly small in comparison to λ_0^2 which results in the statement

$$\Delta s = (2m + 1) \frac{\lambda_0^2}{4 \Delta\lambda} \quad (30)$$

Equation (30) states that the contrast of the interference pattern will be worst when the two interferometer arms differ by $(2m + 1) \lambda_0^2 / 4 \Delta\lambda$.

Now the question is what the optical path difference $\Delta(\Delta s)$ from one contrast disappearance to the next is (i.e., from the m^{th} to the $(m + 1)^{\text{th}}$ order). This is given by

$$\Delta(\Delta s) = (2m + 3) \frac{\lambda_0^2}{4 \Delta\lambda} - (2m + 1) \frac{\lambda_0^2}{4 \Delta\lambda} = \frac{\lambda_0^2}{2 \Delta\lambda} \quad (31)$$

Thus, we can determine the difference of the two wavelengths in the following way: First, search for the mirror position where the interference pattern shows a minimum contrast. Next, move the mirror until you see the next minimum in the contrast. The mirror movement corresponds to $\Delta(\Delta s)/2$. The difference in the wavelength $\Delta\lambda$ can then be determined by

$$\Delta\lambda = \frac{\lambda_0^2}{2 \Delta(\Delta s)} \quad (32)$$

In this kit, the laser features several spectral lines. By observing the fringe contrast, their spectral distance $\Delta\lambda$ can be measured, see Chapter 7.

⁷ Note: The contrast drops to zero which means that no fringes are visible, only a homogeneous intensity distribution on the screen. So naturally, the intensity itself doesn't drop to zero.

Chapter 7 Experiments and Examples

This chapter discusses the various experiments that can be performed with this experiment package. Numerical examples that can be expected under realistic conditions are provided as well.

7.1 Preliminary Tests

Assemble the Michelson interferometer if you have not already done so.

Experiment 1: Change the length of an interferometer arm by moving a mirror (the one in the kinematic holder). What is the effect on the interference pattern?

Sample result:

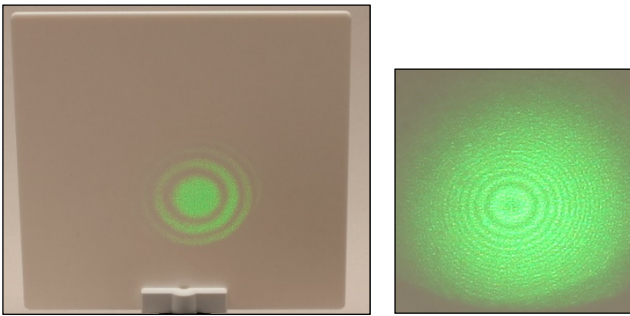


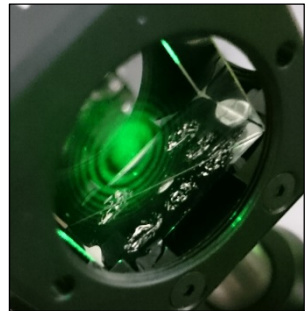
Figure 17 When the interferometer arms have about equal length, the fringes are large. The pattern becomes smaller as the difference in length between the arms increases. See theory section for an explanation.

Experiment 2: Light a match or lighter and put it right below the laser beam in one arm. What do you observe?

Execution: The hot air has a different refractive index than the air at room temperature. Thus, the optical path changes in one arm of the interferometer, causing the interference pattern to shift. Surprisingly, this does not result in a blurred pattern. Instead, the pattern is compressed or stretched and/or moved.

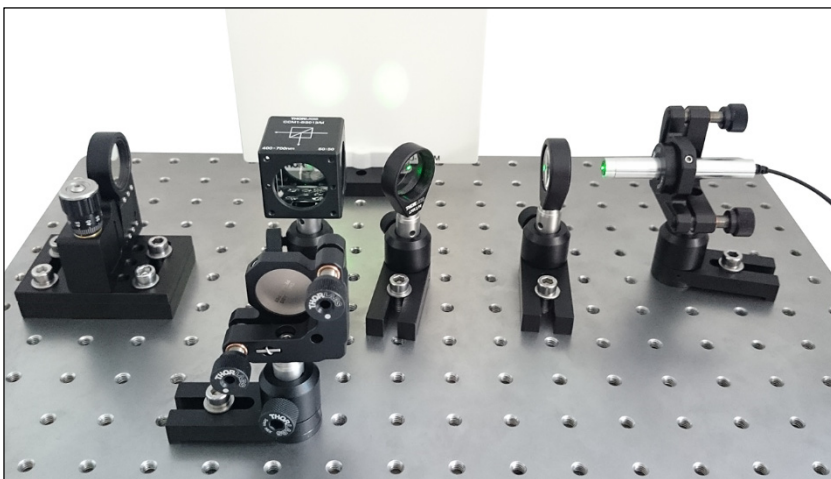
Experiment 3: Verify that a Michelson interferometer has two outputs. Compare both patterns.

Execution: It is important to recognize that the output pointing towards the screen is not the only output of the interferometer. In fact, the second output points towards the laser. It can be observed by looking at the face of the beamsplitter oriented towards the laser, where you can observe an interference pattern as well. Alternatively, put a piece of paper between lens and beamsplitter (without blocking the incident laser beam).



Note: Observing the pattern on the beamsplitter requires a dark room with very little stray light.

Finally, place the second beamsplitter (use one of the post holders from the LED assembly) between the cube beamsplitter and the lens. The newly introduced beamsplitter will also reflect a fraction of the laser light towards the experimenter. Make sure to take care of the unwanted reflections and block the beam accordingly.



This setup allows the two outputs to be observed on the same screen. An example is shown to the right. The light coming from the second beamsplitter has a lower intensity since only 50% is reflected to the screen, the other 50% is transmitted towards the laser.



The key aspect to notice here is that the two patterns are complementary, meaning that the left shows constructive interference where the right shows destructive interference and vice versa. This also clearly shows that the term “destructive interference” does not imply a loss of energy. The light is simply found in the other output.

7.2 Determining the Laser Wavelength

One typical application of an interferometer is to determine the wavelength of the incident light. This measurement is performed through controlled shifting of one mirror, which causes a change in the interference pattern. Depending on the direction the mirror is moved relative to the second mirror, the concentric circles either expand out from the center (with new ones constantly appearing in the center) or they shrink into the center (where they disappear).

Imagine that there is constructive interference in the center, so that the path length difference between the interferometer arms on the optical axis is a multiple of the wavelength. When the mirror is shifted forward by *half the wavelength*, the optical path length difference of both arms has changed by a *full wavelength* since the light passes through each arm on the way there and on the way back. Accordingly, constructive interference is again visible in the center. *This means that shifting the mirror by half the wavelength generates a light-dark-light transition.*

Experiment 4: Determine the wavelength of the laser through translation of the mirror.

Execution: The interferometer is adjusted so that the interference pattern is neither too large nor too small to count the light-dark-light transitions easily. Then the micrometer screw on the mirror positioning stage is turned, which changes the interference pattern. The wavelength is derived from the start and end values of the micrometer screw and the number of dark-light-dark transitions. **One scale division of the micrometer screw corresponds to one micrometer.** Observing numerous transitions is recommended in order to minimize the error.

Tip: This experiment is very good for demonstrating that an interferometer is a very accurate and sensitive measuring instrument. Even a slight touch by hand potentially results in a fluctuation of the pattern. After performing the measurement by hand, insert an Allen key into the screw of the mirror translator and only turn the Allen key.

Tip: While taking measurements, the mirror's direction of translation should not be reversed due to possible backlash of the stage. Do not reverse the direction of rotation of the knob while measuring.

Example: The following values were determined by students in practical tests. The reference value of the laser wavelength is 532 nm.⁸

Number of Transitions	Mirror displacement (μm)	Calculated Wavelength	Error (%)
40	11.2	560 nm	5.3
60	17	567 nm	6.6
80	22	550 nm	3.4

⁸ See also the individual spec sheet of the laser.

The average error in our testing was about 5%. This is due to the fact that counting errors occur, that there is a certain error in reading the micrometer and that the stage's accuracy is limited to a few percent.⁹

7.3 Using the Interferometer as a Spectrometer

Experiment 5: Adjust the interferometer such that the fringe contrast is very low. Next, move the mirror to find the next minimum in the fringe contrast. Use the measured mirror displacement to estimate the difference between peak wavelengths in the emission profile of the laser.

Execution: First, screw in the micrometer screw of the SM1ZP(/M) as far as possible. Then, place the mirrors such that the contrast of the interference fringes is low. Rotate the knob of the SM1ZP(/M) until the contrast has reached a minimum. Then, turn the knob until you've reached the *next* minimum. The difference between good contrast and poor contrast is shown in the following photos:

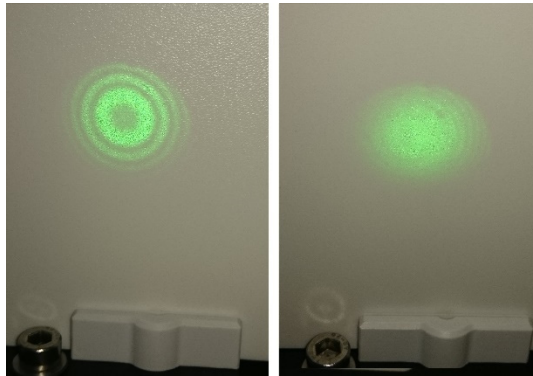


Figure 18 Interference fringes with good contrast (left) and poor contrast (right).

In our test measurements, the transition from good to poor contrast corresponded to a mirror travel range of about 1 mm (equal to 20 full rotations of the knob). This means that the path length difference from one contrast minimum to the next is about $\Delta(\Delta s) = 2$ mm, see Section 6.6: Using the Interferometer as a Spectrometer. According to Equation (32) and a wavelength $\lambda_0 = 532$ nm, this results in a wavelength splitting of 0.07 nm.

This is consistent with the specifications of the CPS532-C2 laser diode. Figure 19 shows an example of a typical spectrum (taken from www.thorlabs.com).¹⁰

⁹ For a more precise measurement, we recommend using piezo crystals, see Chapter 10: Ideas for Additional Experiments.

¹⁰ The laser's spec sheet will only show one peak. This is due to the fact that the spectrum's purpose is just to show the diode's center wavelength.

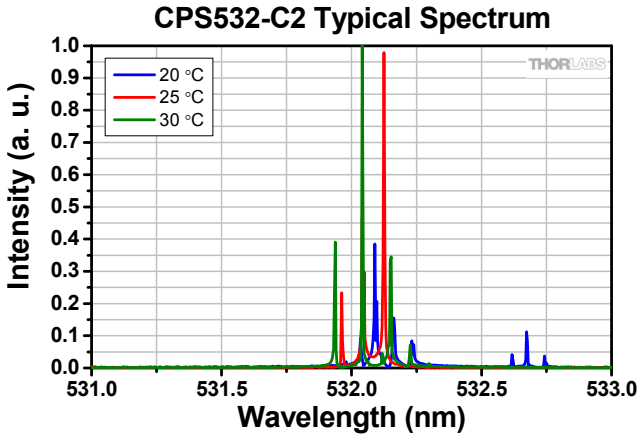


Figure 19 Typical spectrum of a CPS532-C2 laser diode. The spectral composition of the light varies strongly with changing temperature of the housing.

The temperature of the housing will be different from the room temperature. Also, please note that the derivation of Equation (32) assumes two spectral components of equal intensity. This is not the case here since we have more than two components and differing intensities. This also explains why the interference pattern doesn't fully vanish.

While the final result does not provide a complete quantitative measurement of the laser's spectrum, the exercise demonstrates that an interferometer can in fact be used as a spectrometer and that its sensitivity is very high.

7.4 Interference with LEDs, Coherence

In order to see interference with LEDs, one has to adjust the interferometer so that both arms have almost the same length. If the length of the arms differs significantly so that the coherence length of the LEDs is exceeded, no interference will be observed. A preliminary adjustment with the laser is necessary so that the mirror positions needed to observe interference with the LED are easier to find.

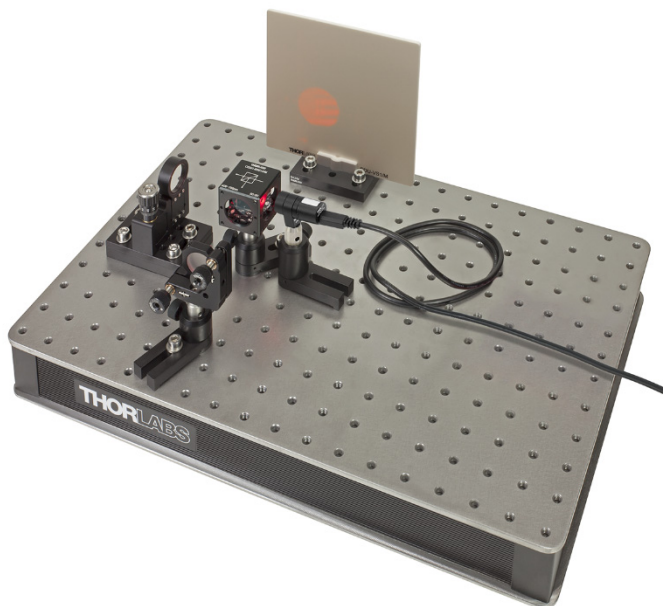
Experiment 6: Use the laser as the light source initially. Adjust the interferometer so that the arm lengths are almost identical.

Execution: Shift one of the mirrors so that the central maximum of the interference pattern gets as large as possible. The central maximum should cover nearly all of the illuminated area on the screen. Only then is the preliminary adjustment good enough to proceed to aligning the setup to observe interference with an LED. This step will require several iterations using the mirror in the kinematic holder.

Experiment 7: Connect the red LED and use it instead of the laser. Now move the mirror until you see an interference pattern.

Execution: The chances of seeing an interference pattern directly after installing the LED are very low. Shift the translatable mirror to find the interference pattern. If you reach the

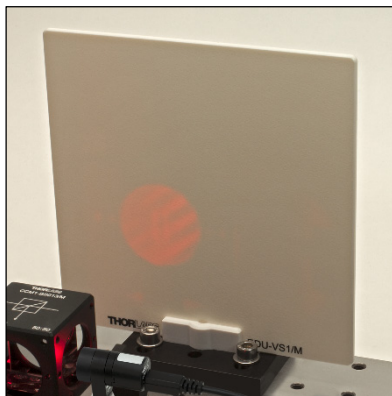
end of the mirror's translation range without finding a pattern, shift it to the other end. If you have not found a pattern along the entire translation range of the mirror, the preliminary adjustment with the laser was not accurate enough. In this case repeat the alignment process with the laser.



Tip: Do not turn the screw too quickly and, when changing your grip, wait briefly to see if an interference pattern develops (~1/2 second) – otherwise you might miss the correct mirror position.

Tip: Place the LED close to the beamsplitter to avoid losing too much intensity.

Tip: As a result of the high divergence of the LED, unwanted reflections at the edges of the beamsplitter and transmission through the holes of the beamsplitter housing can lead to vertical stripes and dots overlaid on the interference pattern. In Chapter 12, we describe measures to avoid this.



Experiment 8: Measure the approximate coherence length of the red LED.

Execution: Shift the mirror until the contrast of the interference pattern has decreased significantly but the pattern can still be observed, and make note of the mirror position.

Then shift the mirror in the other direction, also until the contrast of the interference pattern has decreased significantly. The coherence length is approximately equal to the distance between the two mirror positions where interference is still visible.

Sample result: The result of a test measurement was approximately $25\ \mu\text{m}$. Examining the spectrum in the datasheet for the LED (see Figure 20) one can read the spectral width at half the maximum intensity (FWHM) to be approximately $20\ \text{nm}$. The peak wavelength is about $640\ \text{nm}$. With Equation (13), this results in a theoretical coherence length of $20.5\ \mu\text{m}$.

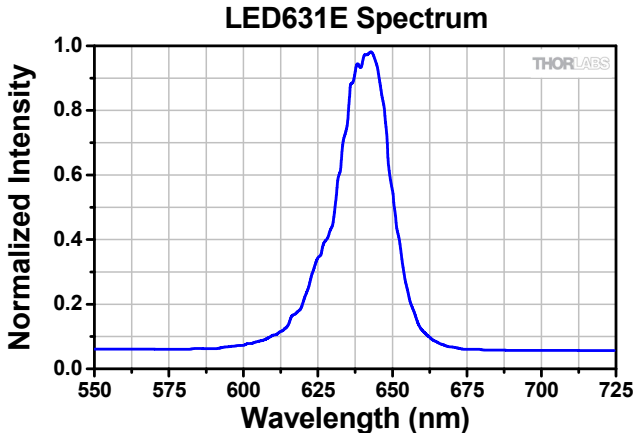


Figure 20 Example spectrum of the red LED from its datasheet.

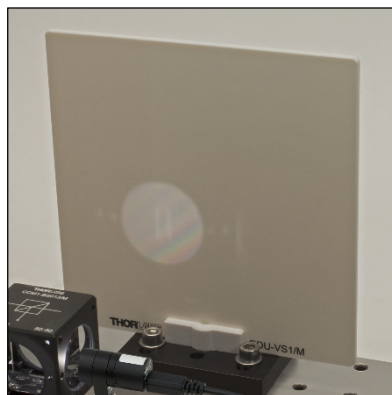
However, it has to be noted here that the coherence length can only be determined in terms of magnitude: first of all, determining it from the interference pattern is already problematic since the contrast can only be estimated by eye. The reference value of the LED is not distinct either, since the wavelength of the maximum and the breadth of the spectral distribution differ slightly for every LED.

Experiment 9: Once you have found the correct position from experiment 8 for red interference, you can replace the red LED with the white one in order to find the mirror position to observe white light interference (it's within the range for the red light interference). Adjust the mirror angle to observe the pattern.

Experiment 10: Measure the approximate coherence length of the white light LED and compare it to the red LED.

Execution: Follow the steps outlined for Exercise 8.

Sample result: The result of a test measurement was approximately $10\ \mu\text{m}$. Due to the broader spectrum of the white LED, the coherence length is smaller compared to the narrower band red LED.



7.5 Refractive Index Determination

In this experiment, we use the interferometer to determine the refractive index of Plexiglas. The theoretical basis for this has already been discussed in Chapter 6. A rotation of the Plexiglas plate in the beam lengthens the optical path and leads to a change in the interference pattern. Together with the rotation angle and the plate thickness, the refractive index can be derived using Equation (20).

Experiment 11: Set the rotation platform with the Plexiglas plate in one arm of the interferometer, replace the LEDs with the laser again and establish an interference pattern, as shown in Figure 21. Adjust the plate so that it stands perpendicular to the beam.

Execution: For starters, the interference pattern should be adjusted so that it is of medium size and the transitions can be readily observed (with the Plexiglas plate in the beam).

Tip: First be sure you understand how the rotation platform functions. When the small set screw at the front is tightened, the entire platform is turned by the fine adjustment screw (See Figure 21). If the set screw is not tightened, the fine adjustment screw does not engage and one can rotate the platform manually by greater angles.

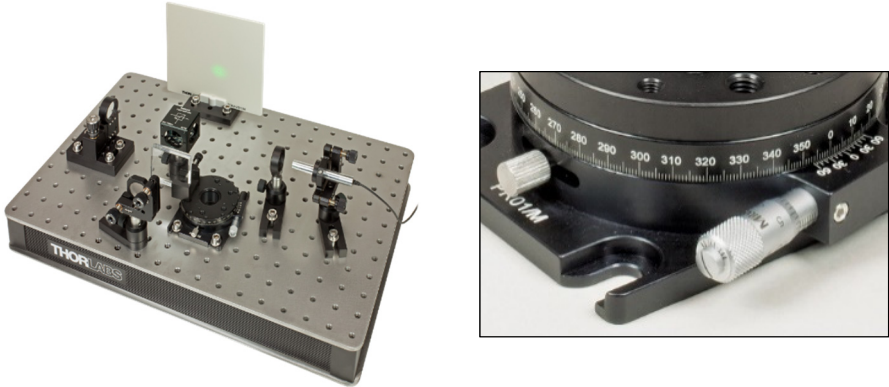


Figure 21 The setup for measuring the refractive index of Plexiglas (left) and the micrometer drive (fine adjustment screw) and locking setscrew on the rotation platform (right). When the setscrew is locked, the fine adjustment is engaged. The stage is then rotated by turning the micrometer drive.

First, loosen the set screw and turn the fine adjustment screw as far in as possible. Now the correct starting point for the measurement still has to be found, i.e. the plate must be positioned so it is precisely perpendicular to the beam. In order to do so, first remove the lens from the setup. You will now probably see more than one spot on the screen due to the reflections of the laser at the air-Plexiglas boundary. Rotate the stage until the spots lie on top of each other (or are parallel if there's also a slight tilt). Now the plate is perpendicular to the beam.

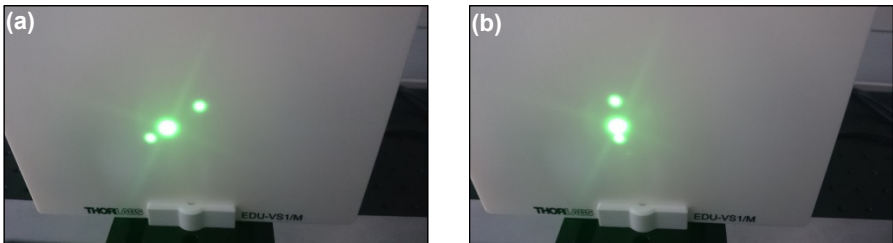


Figure 22 Position of spots on the screen when the Plexiglas plate (a) is not perpendicular to the beam and (b) is perpendicular to the beam.

Experiment 12: Determine the refractive index of Plexiglas by rotating the thin plate.

Execution: After the adjustment from Experiment 11, the measurement can begin – in order to do so, replace the lens, lock the center screw of the stage to engage the fine adjustment screw and note the starting angle on the scale. Turn the fine adjustment screw while counting the number of light-dark-light transitions. At the end of the measurement, read the rotation angle and measure the thickness of the Plexiglas plate. There is a Vernier scale on the platform to aid in precisely reading the angle.



Sample result: The following values were determined by students in practical tests. The reference value for the refractive index n of the Plexiglas plate that was used is 1.49.

Number of Transitions	Rotation Angle	Plate Thickness (mm)	n According to Equation (20)	Error (%)
30	4° 25'	8	1.50	1.0
60	6° 15'	8	1.50	0.9
30	3° 50'	12	1.42	4.6
60	5° 15'	12	1.46	1.8

Experiment 13: Perform the same experiment with the thick plate. How do things change?

Execution: It's the same as before; sample results are found in the table above. The difference between the two scenarios is that the optical path changes more quickly with the thicker plate. Thus, a smaller rotation angle is needed to achieve the same amount of fringe transitions. However, this means that a difference in adjustment has a higher error. Thus, the error for the thick plate is higher than for the thin plate.

Note: The value can be determined with a higher accuracy when more data is acquired. For example, record the rotation angle after 2 steps of light-dark-light transitions. Then, fit the theoretical curve to the numerical data. With this method, the thickness of the plate can also be left as a parameter to be fit.

7.6 Thermal Expansion Coefficient

Experiment 14: Remove the rotation platform from the setup and replace the moveable mirror with the setup to measure thermal expansion (as shown in Figure 23). Adjust the interference pattern again so that you can count the transitions easily.

Experiment 15: Start a controlled heating of the post by applying an external voltage to the heater. Count the number of transitions during expansion and make note of the respective temperature. Derive the expansion coefficient of aluminum.

Execution: Apply an external voltage to the two **outer** contacts of the heater by using the pre-attached banana plug cables and your power supply of choice (up to 12 V with 2 A¹¹). The heater will increase the rod temperature, causing the rod to expand and shift the mirror; this causes a number of fringe transitions that can be observed on the screen and counted. Make sure you give the system enough time to reach thermal equilibrium before increasing the voltage. The temperature is taken by inserting the supplied measurement head of the thermometer into the rod. When the pattern does not change any more, proceed to the next voltage step.



Figure 23 Setup to Determine the Coefficient of Thermal Expansion

Please note that the supplied flexible foil heater with thermistor and banana plugs was chosen as a cost effective combination under the assumption that a standard controllable power supply is available. Thorlabs offers more sophisticated heater controllers, allowing for direct temperature feedback by making use of the thermistor sensor on the foil heater, e.g. the TC200(-EC) benchtop controller or the TTC001 compact controller. Those require different contacting of the heater and thermistor wires of the foil heater. Please refer to our website for more information on our resistive heaters and thermistors:

https://www.thorlabs.com/newgrouppage9.cfm?objectgroup_id=305

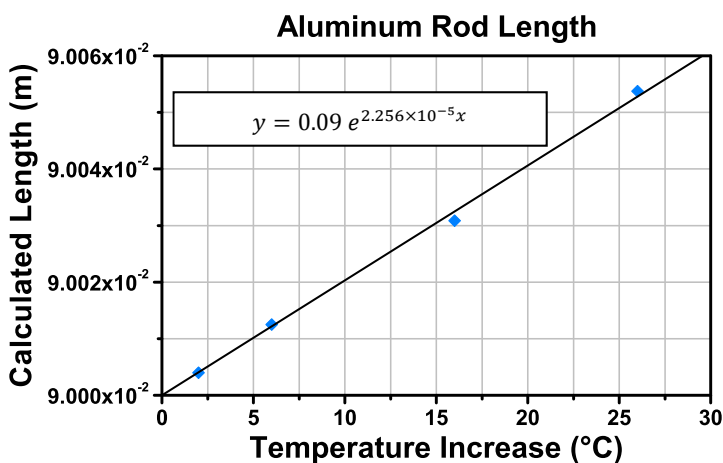
¹¹ The heating power is 10 W/in² at 70°C. With an effective heating area of 2.23 in², this requires an input power of about 23 W.

Sample result: The following values were determined by students in practical tests.

Voltage (V)	Temperature Start (°C)	Temperature End (°C)	ΔT (°C)	# of Fringes in the ΔT -Interval	Total # of Fringes N	Calculated Length (cm)
5.1	24	26	2	15	15	9.0004
7	26	30	6	32	47	9.0013
9	30	40	16	69	116	9.0031
11.2	40	50	26	86	202	9.0054

The last column was calculated as $9 \text{ cm} \cdot 532 \text{ nm} \cdot N/2$. The length of the rod is 9 cm and it's made of aluminum. The factor 1/2 is due to the fact that the light travels to and from the attached mirror. Thus, an expansion of $532 \text{ nm}/2 = 266 \text{ nm}$ results in one bright-dark-bright transition on the screen.

Plotting the calculated length over the increase in the temperature of the rod yields this graph:



Following Equation (22) we can deduce the thermal expansion coefficient to be $\alpha = 2.26 \cdot 10^{-5} \frac{1}{K}$ which is about 2.2% away from the reference value of $2.31 \cdot 10^{-5} \frac{1}{K}$.

Chapter 8 Experiment Overview

Preliminary Tests and Determining the Laser Wavelength

1. Set the Michelson interferometer up and adjust it.
2. Change the length of an interferometer arm by moving the mirror (the one in the kinematic holder). What is the effect on the interference pattern?
3. Light a match or lighter and put it right below the laser beam in one arm. What do you observe?
4. Verify that a Michelson interferometer has two outputs. *Compare both patterns.*
5. Determine the wavelength of the laser through translation of the mirror.

Using the Interferometer as a Spectrometer

6. Adjust the interferometer so that the fringe contrast is very low. Next, move the mirror to find the next minimum in the fringe contrast. Use the measured mirror displacement to estimate the difference between peak wavelengths in the emission profile of the laser.

Interference with LEDs

7. Use the laser as the light source initially. Adjust the interferometer so that the arm lengths are almost identical.
8. Connect the red LED and use it instead of the laser. Now shift the mirror until you see an interference pattern.
9. Measure the approximate coherence length of the red LED.
10. Once you have found the correct position from experiment 4 for red interference, you can replace the red LED with the white one. Then find the white light interference position, which will lie within the range for the red light interference.
11. Measure the approximate coherence length of the white light LED and compare it to the red LED.

Refractive Index Determination

12. Set the rotation platform with the Plexiglas plate in one arm of the interferometer, replace the LEDs with the laser again and establish an interference pattern. Adjust the plate so that it stands perpendicular to the beam.
13. Determine the refractive index of Plexiglas by rotating the thin plate.
14. Perform the same experiment with the thick plate. How do things change?

Thermal Expansion Coefficient

15. Remove the rotation platform from the setup and replace the moveable mirror with the setup to measure thermal expansion. Adjust the interference pattern again so that you can count the transitions easily.
16. Start a controlled heating of the post by applying an external voltage to the heater. Count the number of transitions during expansion and make note of the respective temperature. Derive the expansion coefficient of aluminum.

Chapter 9 Questions

This list of questions also provides a starting point for topics that can be examined in relation to the Michelson interferometer (even beyond this experiment package).

- What is the difference in the interference patterns when the arms are (a) of the same length and (b) of different lengths?
- How many outputs does a Michelson interferometer have?
- When the mirror is shifted and a light-dark-light transition is observed in the interference pattern – by what path length was the mirror shifted?
- Why is it best to use a laser as the light source in an interferometer and not an incandescent lamp?
- How were interference experiments conducted before lasers were invented?
- What is the most well-known experiment in which a Michelson interferometer was used? What was it intended to demonstrate?
- What is the difference between the spectrum of the red LED and the white LED? What effect does this have on the coherence length?
- Instead of a beamsplitter cube, one can also use a plate beamsplitter. However, one needs a compensator plate in one of the interferometer arms.
 - What is the purpose of the compensator plate?
 - Why is it not needed when a cube beamsplitter is used?
 - Can the effect of the compensator plate also be achieved by merely shifting one of the mirrors?
- The interference pattern of the red LED shows red, concentric circles. Why are no white concentric circles seen with the white light LED?
- Instead of using the rotation method, the refractive index can also be determined approximately with the help of white light interference. So, if one does not have a rotation platform: how does one proceed with white light interference in order to determine the refractive index?
- How does the calculation of the thermal expansion coefficient change when the metal rod is not clamped at the end but in the middle?
- When the rod is heated, the interference rings sometimes shrink into the center and sometimes expand out of the center. Why? More precisely: how do the arm lengths have to be adjusted so that the rings expand out of the center (or shrink into the center)?

Chapter 10 Ideas for Additional Experiments

Beyond the phenomena described in this experiment package, a Michelson setup offers numerous other opportunities for the exciting study of physics. Here is a collection of a few ideas for how the setup can be expanded in case of further interest.

- **Mirror Translation with Piezo Crystals**

In this kit, the mirror is moved manually using a screw. Using a piezo crystal makes much finer adjustments possible. Such a crystal expands in a defined way when an external voltage is applied. As a result, the translation of the mirror can be controlled with great precision in increments smaller than 50 nm. Since piezo crystals are widespread in modern nano-positioning systems, their use offers a learning experience with broad applications.

One possible setup using Thorlabs components could comprise a kinematic holder with support arm [KM100PM(/M), PM3(/M)], a mirror (e.g., ME1S-G01), a Piezo stack (such as AE0203D08) and a KPZ101 Controller.

However, piezo crystals exhibit hysteresis which means that the actual displacement varies depending on whether the voltage is increased or decreased. To make precise measurements, a feedback mechanism is needed to compensate for the hysteresis. A possible setup comprises a kinematically mounted mirror (e.g., ME1S-G01 in KM100) on a stage [e.g., NFL5DP20S(/M)], a KPZ101 piezo controller and a KSG101 strain gauge reader.

Alternatively, you can use the interferometer to measure the hysteresis curve itself.

- **Refractive Index of Gases**

By counting light-dark-light transitions, one can also derive the refractive index of gases (especially depending on volume and pressure). In order to do so, one loads a closed, evacuated cuvette into the setup and slowly fills it with the gas in question. The change in the optical path results in a corresponding change of the interference pattern.

- **Decreased Coherence Length of Lasers Below the Lasing Threshold**

If a laser is operated at currents below its threshold current, light is still emitted via luminescence. Compared to actual lasing, this light is of lower intensity and much broader linewidth. Hence, the coherence length is lowered considerably. This effect can be shown with the help of the Michelson interferometer by substituting the CPS532-C2 laser with a laser for which the pumping current can be manually adjusted. An example is the Thorlabs L658P040 Laser Diode in combination with the TLD001 Driver, SR9A-DB9 Mount, and LTN330-A Adjustable Collimation Tube. Two example spectra of this laser at different currents are presented in Figure 24, highlighting the significantly broader emission peak at lower currents. Be aware that the spectra in Figure 24 are normalized for better comparability. On an absolute scale, the intensity for the higher current is more than an order of magnitude higher than for the lower current. The reduced coherence length resulting from the broader peaks can be

measured with the Michelson Interferometer just as described for the LEDs in Chapter 7.4. Our test measurements have yielded coherence lengths between $20\ \mu\text{m}$ and $400\ \mu\text{m}$ for currents between 19 mA and 38 mA, which are in acceptable agreement with the values calculated from the spectra (see Figure 25). For the calculation, Gaussian peaks have been approximated, which explains the deviation to the measured values. Optionally, the economy beamsplitter included in this kit can be applied for simultaneous display of the interference pattern on a screen and the respective spectrum via a spectrometer [e.g. Thorlabs CCS100(M)]. This experiment can also give a deeper understanding of very common laser diodes and their working principle.

Please be aware that the L658P040 and comparable laser sources are class 3B and should only be operated while wearing suitable laser safety goggles.

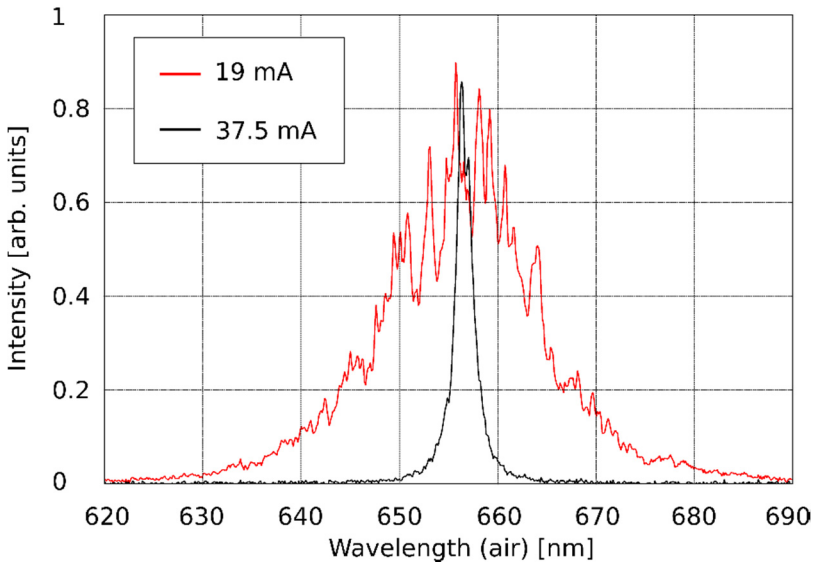


Figure 24 Comparison of L658P040 spectra at different drive currents below the lasing threshold. Spectra are normalized for comparability (absolute values for peak intensity differ by more than one order of magnitude).

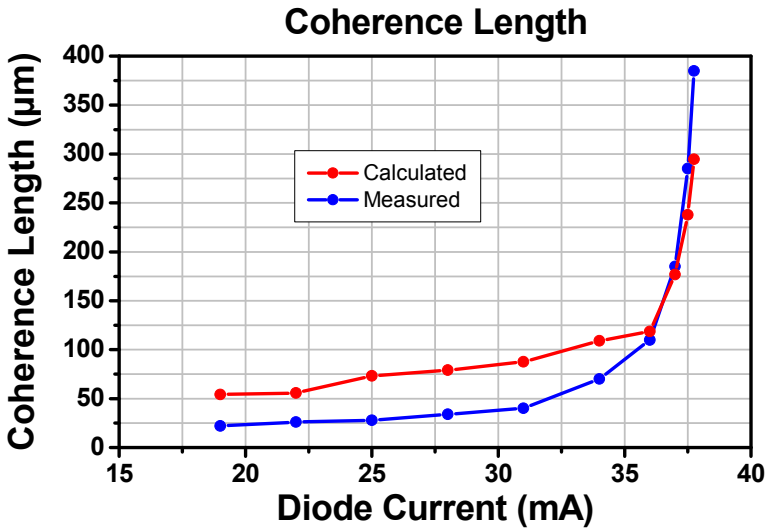


Figure 25 Coherence lengths for different diode currents as measured via Michelson interferometry and as calculated from the spectra.

- **Adjustment of White Light Interference via a Spectrometer**

In order to facilitate the adjustment of the Michelson Interferometer especially for white light interference, a spectrometer (e.g. Thorlabs CCS100) can be used instead of the naked eye. Then, one replaces the screen by the light collection element of the spectrometer and views the spectrum with a suitable software. At an optical path length difference below 600 µm, one will begin to see ripples in the spectrum, which become wider and more pronounced as the path length difference is reduced. The reason for this behavior are the different interference conditions for different wavelengths, some of which interfere destructively. Let λ_n be a wavelength at which destructive interference occurs, and λ_{n+1} be the next higher wavelength fulfilling the same condition. The spectral distance $\Delta\lambda_n = \lambda_{n+1} - \lambda_n$ between the two wavelengths depends only on λ_n and the path length difference of the interferometer Δs , which is given by the setup. For the case of $\Delta s > \lambda_n$, one can calculate $\Delta\lambda_n$ as follows, starting with the phase difference conditions for destructive interference at both λ_n and λ_{n+1} while keeping in mind that for a fixed path length difference the phase difference decreases with increasing wavelength:

Phase difference $\Delta\varphi_n$ for λ_n :
$$\Delta\varphi_n = \frac{2\pi}{\lambda_n} \Delta s = (2n + 1)\pi$$

Phase difference $\Delta\varphi_{n+1}$ for λ_{n+1} :
$$\Delta\varphi_{n+1} = \frac{2\pi}{\lambda_{n+1}} \Delta s = (2n - 1)\pi$$

Subtracting those two equations yields:
$$\frac{1}{\lambda_{n+1}} \Delta s - \frac{1}{\lambda_n} \Delta s = -1$$

Expanding the fractions yields:
$$\frac{\lambda_n}{\lambda_{n+1} \cdot \lambda_n} \Delta s - \frac{\lambda_{n+1}}{\lambda_{n+1} \cdot \lambda_n} \Delta s = -1$$

Further rearranging results in:
$$(\lambda_{n+1} - \lambda_n) \Delta s = \lambda_{n+1} \cdot \lambda_n$$

Substituting $\Delta \lambda_n = \lambda_{n+1} - \lambda_n$ gives:
$$\Delta \lambda_n \Delta s = \lambda_n^2 + \lambda_n \cdot \Delta \lambda_n$$

Additional rearranging yields:
$$\Delta \lambda_n = \frac{\lambda_n^2}{\Delta s - \lambda_n}$$

From the final equation, the two factors determining the spectral distance of neighboring minima become apparent: Firstly, the distance increases towards longer wavelengths and secondly, it increases towards lower path length differences. This means that the ripples in the spectrum become farther spaced and more prominent when reducing the path length difference by moving the translatable of the Michelson interferometer, providing information about the direction and the approximate distance of the mirror movement required to observe white light interference.

Figure 26 shows three example spectra, obtained with a Thorlabs CCS100 spectrometer and the Thorlabs OSA software for a LEDW7E white light LED. The black curve was recorded at large path length differences and thus shows the spectrum of the LEDW7E without any interference effects. The blue and red curves were recorded at path length differences of 600 μm and 15 μm (corresponding to mirror translations of 300 μm and 7.5 μm), respectively. The point of zero path length difference for these measurements is determined by optimal contrast of the white light interference pattern on a screen. As this relies on observation with the naked eye, an error margin of few μm should be assumed. A significant difference between the blue and black curves in Figure 26 is observed, showing that the ripples in the spectrum become observable at path length differences more than 50 times larger than for the white light interference pattern on a screen (ca. 10 μm). Hence, adjusting the mirror position for optimal white light interference becomes easier with the use of the spectrometer. The rippling effect can also be observed for any other LED in the visible spectrum.

For the idea of this additional experiment, we thank Associate Professor Gaël Latour, Université Paris-Sud, Orsay, France.

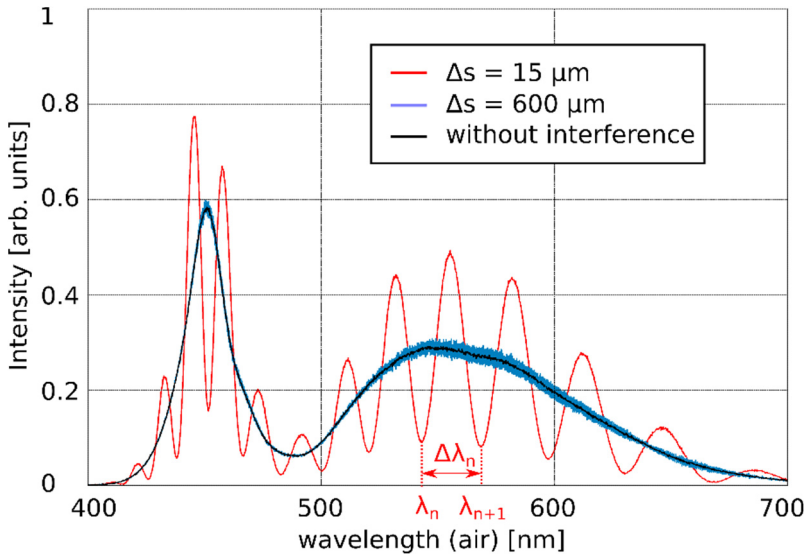


Figure 26 Ripples in the white light spectra of a LEDW7E for path length differences of $15\ \mu\text{m}$ (red), $600\ \mu\text{m}$ (blue), and for very large path differences without interference effects (black). The closer one gets to the point of white light interference, the larger and further spaced the maxima become.

- **Automated Evaluation**

In order to simplify counting the transitions and support a larger number of cycles, it is possible to install a suitable photodetector instead of the observation screen. The advantage of a photodetector is that the voltage values can be recorded using a digital oscilloscope and evaluated without additional software.

A possible setup using Thorlabs components is as follows:

1x **SM05PD1A** Silicon Photo Diode, 1x **SM05D5** Iris, 1x **SM05M10** Lens Tube, 1x **SM05RC/M** Lens Tube Retaining Ring, 1x **CA2812** SMA on BNC Cable, 1x **T3285** BNC T-Piece, 1x **FT104** Termination Resistor, 1x **T1452** Adapter on Banana Plug

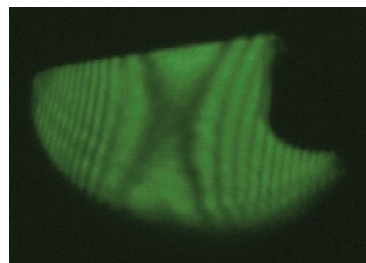
Chapter 11 Modern Michelson Interferometry – LIGO

A recent application of the Michelson interferometer that attracted a lot of international attention is gravitational-wave detection. Gravitational waves are oscillations in space-time curvature produced by colliding black holes, neutron stars, and other astrophysical processes that involve a dense concentration of mass-energy moving at relativistic speeds. A network of laser interferometers has been constructed in several countries to detect these waves. This includes the Laser Interferometer Gravitational-Wave Observatory (LIGO) in the United States, VIRGO in Italy, GEO600 in Germany, and KAGRA in Japan. All of these experiments consist of a Michelson interferometer with kilometer-scale arm lengths. The mirrors are suspended and free to swing in the plane of the interferometer. A passing gravitational wave will shrink the mirror-beamsplitter distance in one arm of the interferometer while stretching that distance in the other arm. The oscillating shrinking/stretching pattern induced by the passing wave is recorded as an oscillating signal in the photodetector. On September 14, 2015 the twin LIGO detectors (in Washington state and Louisiana) made the first direct detection of a gravitational wave. The signal (which was measured with high confidence in both detectors) was produced by an orbiting pair of black holes that merged together about a billion light years away. This signal caused the LIGO mirrors to move by about 10^{-18} meters, or nearly one-thousandth the diameter of a proton. Michelson interferometers can thus perform some of the most sensitive length measurements possible. LIGO and its partner observatories are vastly more complicated than the interferometer in this kit, but the fundamental physical principle behind their operation is Michelson interferometry.¹²

¹² We cordially thank the LIGO collaboration, in particular Marc Favata, Nancy Aggarwal and Maggie Tse, for this addition to the manual.

Chapter 12 Troubleshooting

- *The laser spots superpose, but there is no interference.*
Check whether all of the components have been positioned as precisely as possible (Is there a 90° beam angle after reflection? Is the height of the beam above the plate at the screen the same as it is directly at the laser?). If these conditions exist, you may have to simply experiment a little and slightly change one spot repeatedly without completely losing the superposition.
- *You have found an interference pattern, but the diameter is very small.*
If this is the case, it is probable that the distance between the beamsplitter and the mirror in one of the arms of the interferometer is much greater than in the other arm. Therefore, move the mirror so that the distances are as equal as possible.
- *The interference sometimes disappears for no apparent reason without the setup being touched.*
Temperature changes in the crystal can lead to changes in the laser modes. Place a hand on the laser module and warm it slightly – the interference should appear again.
- *The contrast of the interference pattern varies.*
One reason is the temperature change mentioned in the previous point. However, the fringe contrast/visibility also changes when there is more than one line in the spectrum of the used laser which is the case for the CPS532-C2. So the variation of the visibility is nothing to be concerned about and can actually be used for precision spectroscopy, see Chapters 6.6 and 7.3. Simply move one mirror which should increase the contrast.
- *Instead of the ring-shaped interference pattern, hyperbolic-shaped interference fringes can be seen.*
These and other distortions of the interference pattern typically occur when the height of the beams along both arms of the interferometer is not exactly the same. We recommend moving the screen along the beam to check the heights throughout the setup.
- *No red light / white light interference can be found.*
It is important to first adjust the interferometer with the laser so that the arm lengths are effectively equal. Due to the low coherence of LED light, the arms ultimately have to correspond within a few dozen micrometers. In order to achieve this, the post-mounted mirror should be fine-tuned so that the visible interference pattern (when using the laser!) consists almost exclusively of the central maximum. Only then is the preliminary adjustment good enough to



proceed with fine-tuning using the red LED and the moveable mirror. When the LED is in the setup, the mirror has to be shifted until interference can be observed. If no interference can be observed along the entire translation path of the mirror, the preliminary adjustment has to be repeated and if possible refined.

- *Vertical stripes and dots occur in or near the interference pattern when operating with the LED.*

These are caused by light reflected at the edges of the beamsplitter or passing through the housing of the beamsplitter because of the large divergence of the LED. Sealing the small holes in the housing of the beamsplitter cube with e.g. black tape avoids the dot-like artifacts. In order to get rid of the vertical stripes, we recommend screwing an SM1RR Ø1" retaining ring into the thread of the cube housing on each of the two mirror-facing sides. This reduces the diameter of the opening and avoids illumination of the cube edges.

- *The thermal expansion is too fast or the calculated values for the coefficient deviate too much from the literature values.*

In these cases the voltage of the heating element should be increased more gradually. In particular, one should give the system some time to reach a thermal balance before reading the temperature. Also, make sure that the rod is fixed at its very end in the 90° angle bracket. Only then the expansion will be fully translated into a mirror movement into the right direction.

Chapter 13 Appendix

Determining the refractive index was discussed in Section 6.4. Here the calculation that leads to equation (20) is presented in detail. The content discussed in Chapter 6 on the physical and optical path is presumed to be known here.

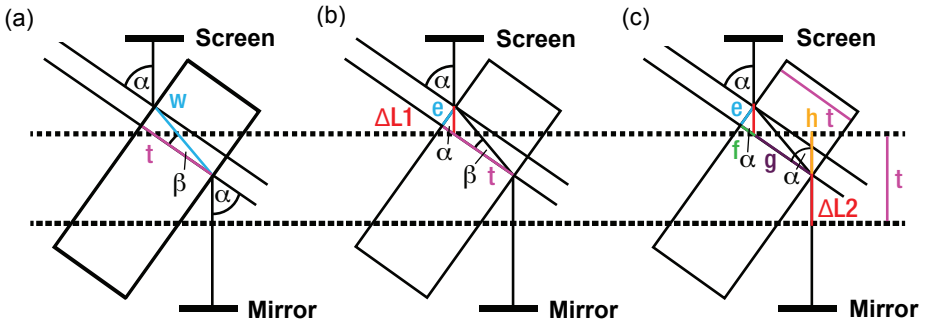


Figure 27 Rotated plate with refractive index n in the beam path

To examine the entire optical and/or physical path, it is best to segment it into three sections as shown in Figure 27(a) through (c). The section in the plate is easy to determine. Figure 27(a) shows that

$$\cos \beta = \frac{t}{w} \Rightarrow w = \frac{t}{\cos \beta} \tag{33}$$

applies. Similarly one sees in Figure 27(b), that

$$\sin \alpha = \frac{e}{\Delta L1} \Rightarrow \Delta L1 = \frac{e}{\sin \alpha} \tag{34}$$

where we make note of the relation

$$e = t \cdot \tan \beta \tag{35}$$

for subsequent steps. Determining $\Delta L2$ is more complex. Note that

$$g = t - f = t - \frac{e}{\tan \alpha} \tag{36}$$

applies, which for h results in

$$\cos \alpha = \frac{h}{g} \Rightarrow h = g \cdot \cos \alpha = \left(t - \frac{e}{\tan \alpha} \right) \cdot \cos \alpha \tag{37}$$

Now $\Delta L2$ can be calculated as

$$\Delta L2 = t - h \tag{38}$$

We now have almost everything we need for equation (20). First we want to point out Snell's law of refraction, according to which

$$1 \cdot \sin \alpha = n \cdot \sin \beta \quad (39)$$

applies, where we assumed the refractive index of air with a good approximation of 1. For a subsequent calculation step, one still needs

$$\cos \beta \stackrel{(31)}{=} \cos \left(\arcsin \left(\frac{\sin \alpha}{n} \right) \right) = \sqrt{1 - \frac{\sin^2 \alpha}{n^2}} \quad (40)$$

where the latter equality is derived from trigonometric calculation rules.

As discussed in Chapter 6, the optical path length difference is then derived from

$$\begin{aligned} N \cdot \lambda &\stackrel{(19),(18)}{=} 2 \cdot (-\Delta L1 + n \cdot w + \Delta L2 - n \cdot t) \\ &\stackrel{(26),(25),(30),(29)}{=} 2 \cdot \left(-\frac{e}{\sin \alpha} + n \cdot \frac{t}{\cos \beta} + t - \left(t - \frac{e}{\tan \alpha} \right) \cdot \cos \alpha - n \cdot t \right) \\ &= 2 \cdot \left(e \cdot \left(\frac{-1}{\sin \alpha} + \frac{\cos \alpha}{\tan \alpha} \right) + n \cdot \frac{t}{\cos \beta} + t - t \cdot \cos \alpha - n \cdot t \right) \\ &\stackrel{(27)}{=} 2 \cdot \left(t \cdot \tan \beta \cdot (-\sin \alpha) + n \cdot \frac{t}{\cos \beta} + t - t \cdot \cos \alpha - n \cdot t \right) \\ &\stackrel{(31)}{=} 2 \cdot t \cdot \left(-\sin \alpha \cdot \frac{\sin \alpha}{n \cdot \cos \beta} + \frac{n}{\cos \beta} + 1 - \cos \alpha - n \right) \\ &= 2 \cdot t \cdot \left((n^2 - \sin^2 \alpha) \cdot \frac{1}{n \cdot \cos \beta} + 1 - \cos \alpha - n \right) \\ &\stackrel{(32)}{=} 2 \cdot t \cdot \left(\sqrt{n^2 - \sin^2 \alpha} + 1 - \cos \alpha - n \right) \end{aligned} \quad (41)$$

Now equation (41) is solved to the root term and squared. We then have:

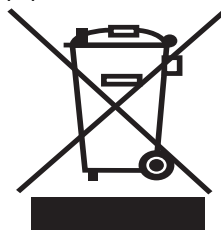
$$\begin{aligned} \left(\frac{N\lambda}{2t} - 1 + \cos \alpha + n \right)^2 &= n^2 - \sin^2 \alpha \\ \Rightarrow \left(\frac{N\lambda}{2t} - 1 + \cos \alpha \right)^2 + n^2 + 2n \cdot \left(\frac{N\lambda}{2t} - 1 + \cos \alpha \right) &= n^2 - \sin^2 \alpha \\ \Rightarrow 2n \cdot \left(\frac{N\lambda}{2t} - 1 + \cos \alpha \right) &= -\sin^2 \alpha - \left(\frac{N\lambda}{2t} - 1 + \cos \alpha \right)^2 \end{aligned}$$

This immediately results in the equation (20) for the refractive index.

Chapter 14 Regulatory

As required by the WEEE (Waste Electrical and Electronic Equipment Directive) of the European Community and the corresponding national laws, Thorlabs offers all end users in the EC the possibility to return “end of life” units without incurring disposal charges.

- This offer is valid for Thorlabs electrical and electronic equipment:
- Sold after August 13, 2005
- Marked correspondingly with the crossed out “wheelie bin” logo (see right)
- Sold to a company or institute within the EC
- Currently owned by a company or institute within the EC
- Still complete, not disassembled and not contaminated



As the WEEE directive applies to self contained operational electrical and electronic products, this end of life take back service does not refer to other Thorlabs products, such as:

- Pure OEM products, that means assemblies to be built into a unit by the user (e.g. OEM laser driver cards)
- Components
- Mechanics and optics
- Left over parts of units disassembled by the user (PCB's, housings etc.).

If you wish to return a Thorlabs unit for waste recovery, please contact Thorlabs or your nearest dealer for further information.

Waste Treatment is Your Own Responsibility

If you do not return an “end of life” unit to Thorlabs, you must hand it to a company specialized in waste recovery. Do not dispose of the unit in a litter bin or at a public waste disposal site.

Ecological Background

It is well known that WEEE pollutes the environment by releasing toxic products during decomposition. The aim of the European RoHS directive is to reduce the content of toxic substances in electronic products in the future.

The intent of the WEEE directive is to enforce the recycling of WEEE. A controlled recycling of end of life products will thereby avoid negative impacts on the environment.

Chapter 15 Thorlabs Worldwide Contacts

For technical support or sales inquiries, please visit us at www.thorlabs.com/contact for our most up-to-date contact information.



USA, Canada, and South America

Thorlabs, Inc.
sales@thorlabs.com
techsupport@thorlabs.com

Europe

Thorlabs GmbH
europe@thorlabs.com

France

Thorlabs SAS
sales.fr@thorlabs.com

Japan

Thorlabs Japan, Inc.
sales@thorlabs.jp

UK and Ireland

Thorlabs Ltd.
sales.uk@thorlabs.com
techsupport.uk@thorlabs.com

Scandinavia

Thorlabs Sweden AB
scandinavia@thorlabs.com

Brazil

Thorlabs Vendas de Fotônicos Ltda.
brasil@thorlabs.com

China

Thorlabs China
chinasales@thorlabs.com



THORLABS
www.thorlabs.com
